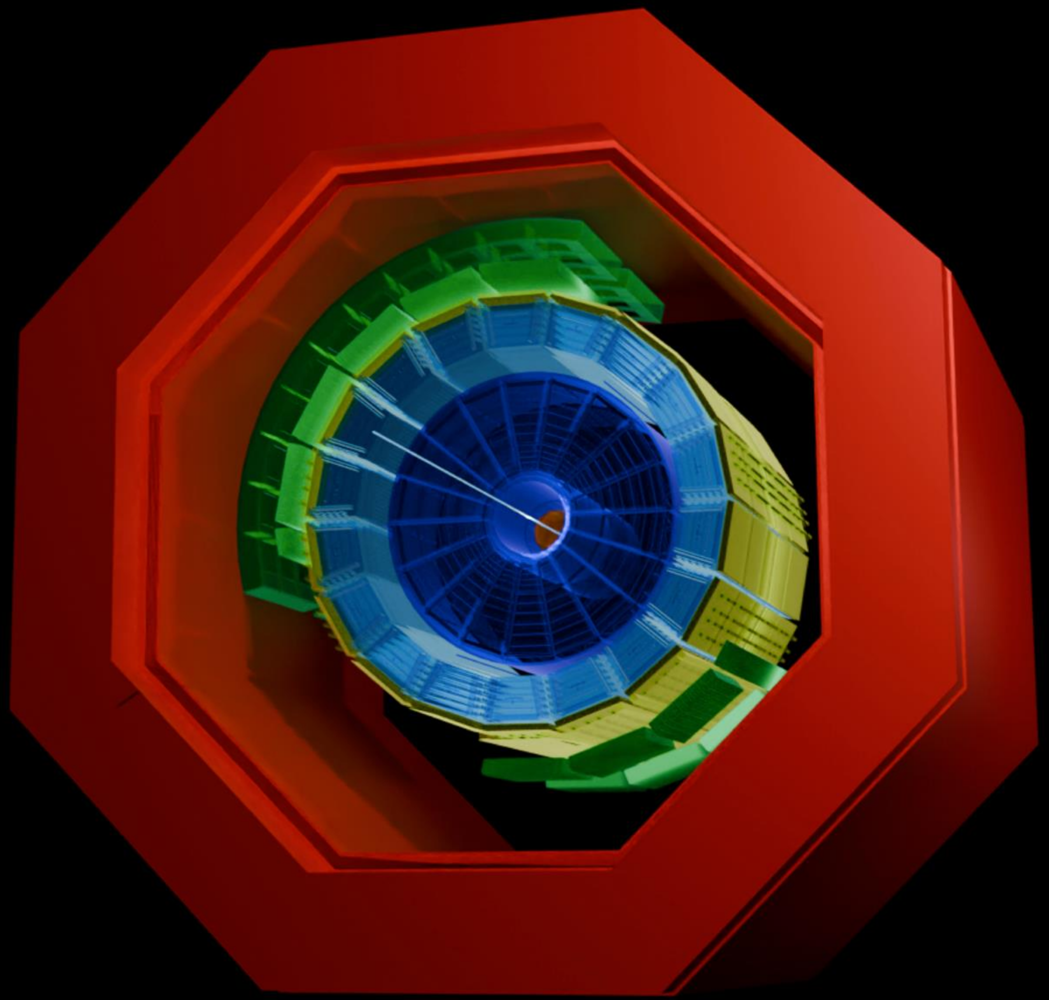

From Protons to Photons Strangeness Production with ALICE at the LHC

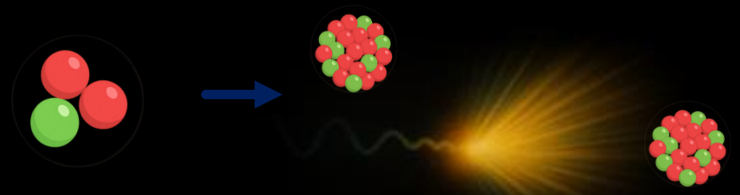

Ph.D. student day 2025

Roman Nepeivoda*
Lund University

December 11th, 2025

LUND UNIVERSITY

ALICE

*roman.nepeivoda@fysik.lu.se

At high temperatures and densities, quarks and gluons are no longer confined into hadrons but behave quasi-freely

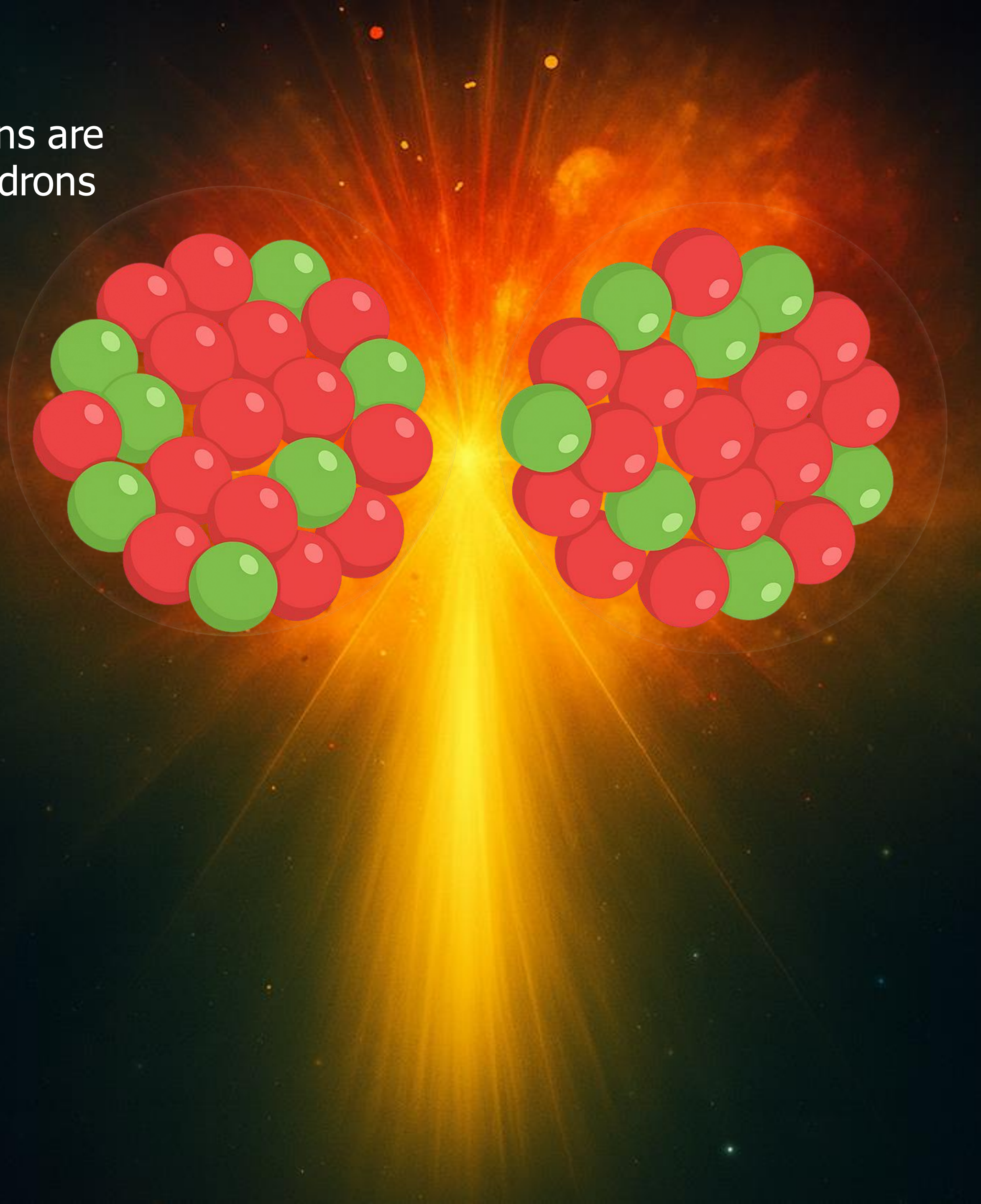

At high temperatures and densities, quarks and gluons are no longer confined into hadrons but behave quasi-freely

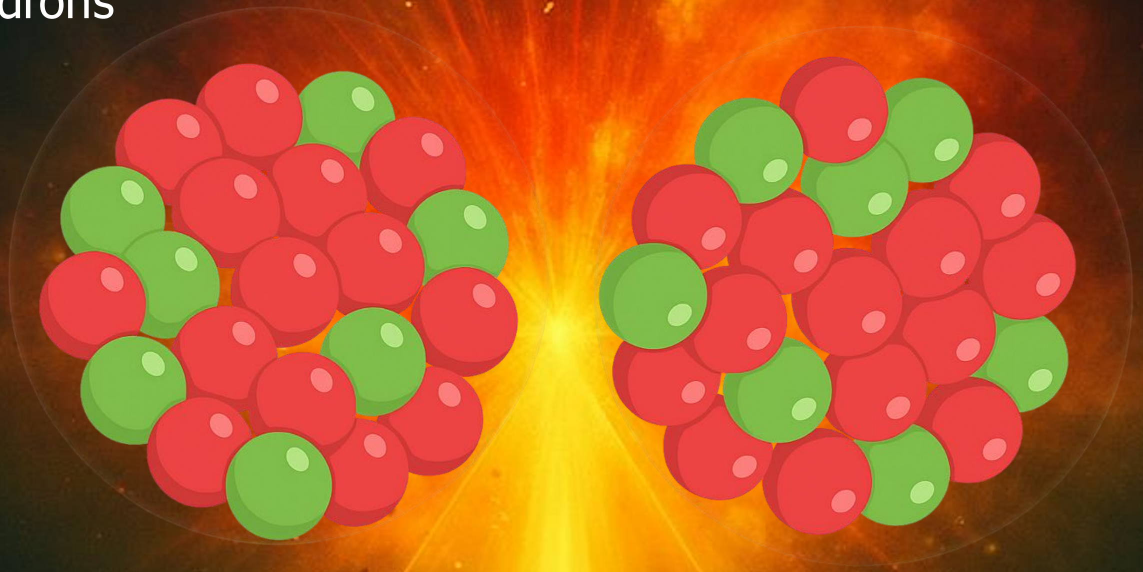

This deconfined state of matter is called the **q**uark–**g**luon **p**lasma (**QGP**)

At high temperatures and densities, quarks and gluons are no longer confined into hadrons but behave quasi-freely

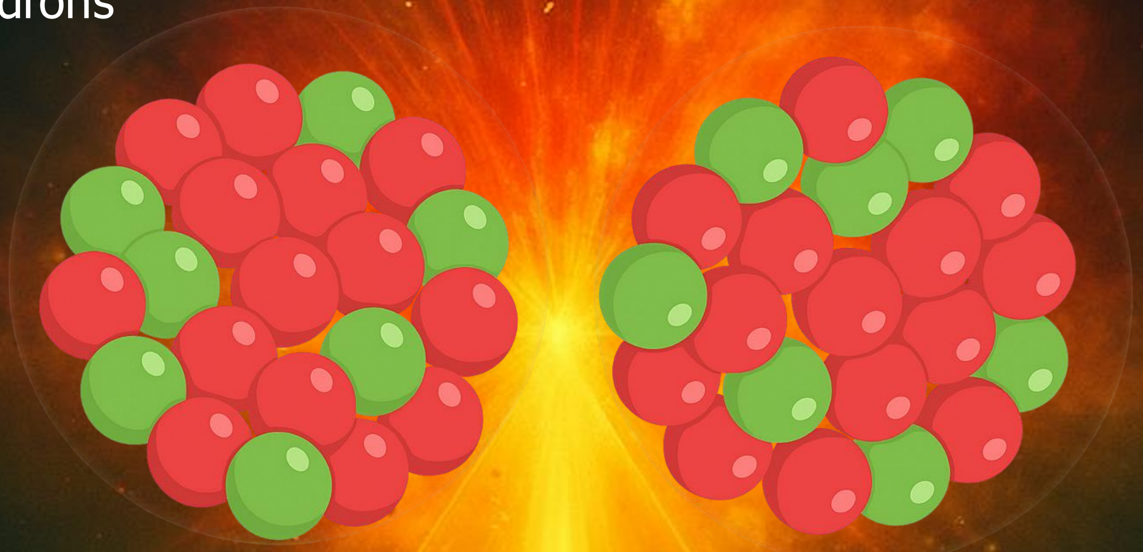

This deconfined state of matter is called the **q**uark–**g**luon **p**lasma (**QGP**)

It existed in the early Universe,
a few microseconds
after the Big Bang
with a temperature at phase transition
$T \approx 2 \cdot 10^{12} K = 200 \text{ MeV}$

At high temperatures and densities, quarks and gluons are no longer confined into hadrons but behave quasi-freely

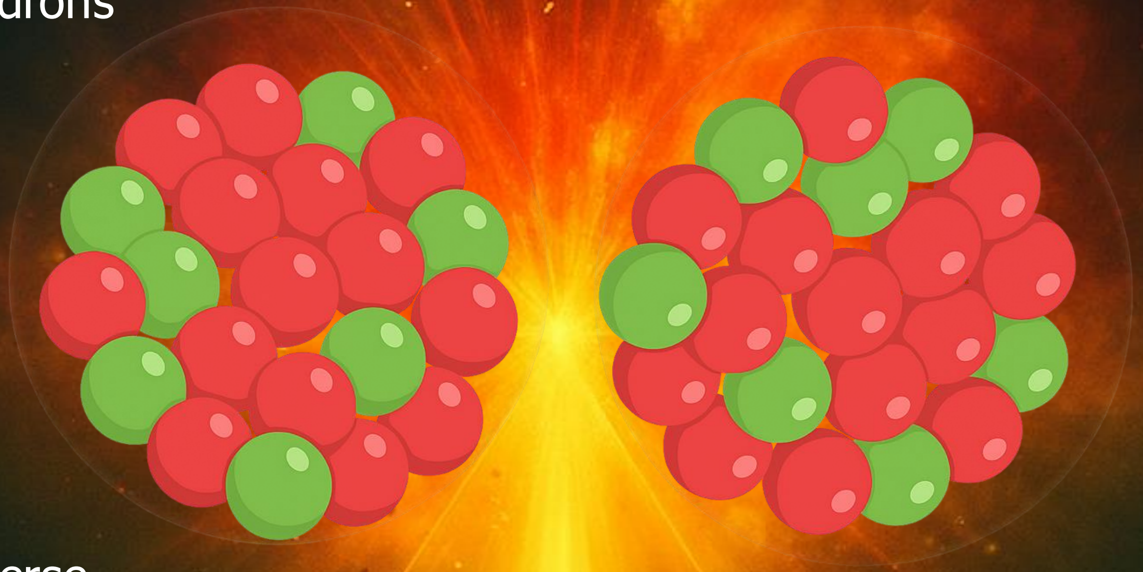

This deconfined state of matter is called the **q**uark–**g**luon **p**lasma (**QGP**)

It existed in the early Universe, a few microseconds after the Big Bang with a temperature at phase transition $T \approx 2 \cdot 10^{12} K = 200 \text{ MeV}$

Heavy-Ion collisions at the LHC recreate the QGP of nuclear size to study its properties and evolution

At high temperatures and densities, quarks and gluons are no longer confined into hadrons but behave quasi-freely

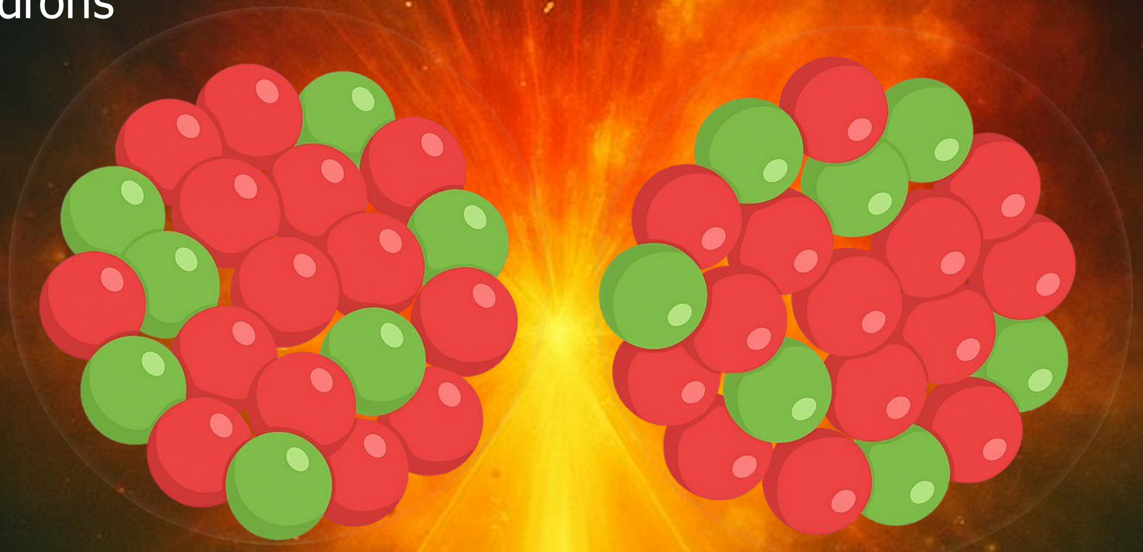

This deconfined state of matter is called the **q**uark–**g**luon **p**lasma (**QGP**)

It existed in the early Universe,
a few microseconds
after the Big Bang
with a temperature at phase transition
$T \approx 2 \cdot 10^{12} K = 200 \text{ MeV}$

Heavy-Ion collisions at the LHC recreate the QGP of nuclear size to study its properties and evolution

Dynamical description of Heavy-Ion collisions from underlying theory of QCD remains an **outstanding challenge!**

ALICE Setup in Run 3

Interaction rate of
500 kHz pp
50 kHz Pb-Pb

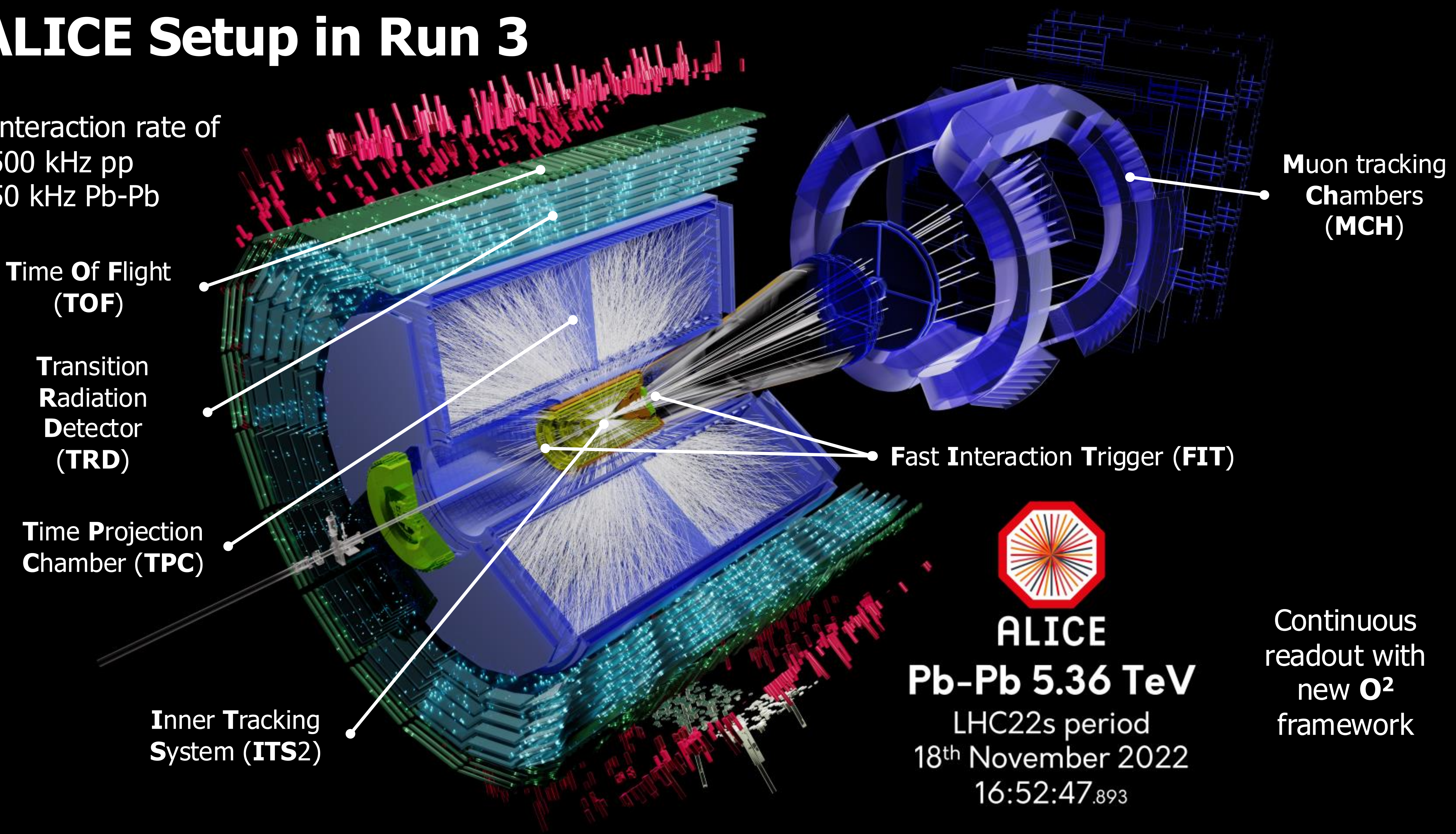

Continuous readout with new O^2 framework

ALICE Setup in Run 3

1. Pseudorapidity (η) is used to represent an angle of a particle relative to the beam axis:

$$y \equiv \frac{1}{2} ln\left[\frac{E + p_{\mathrm{L}}}{E - p_{\mathrm{L}}}\right]$$

$$m \ll |\boldsymbol{p}|$$

$$\eta \equiv -ln\left[tan\left(\frac{\Theta}{2}\right)\right]$$

2. Particle production is often studied as a function of the mid-rapidity charged particle multiplicity:

$$\left\langle {}^{\mathrm{d}N_{\mathrm{ch}}}/_{\mathrm{d}\eta} \right\rangle_{|\eta|<0.5}$$

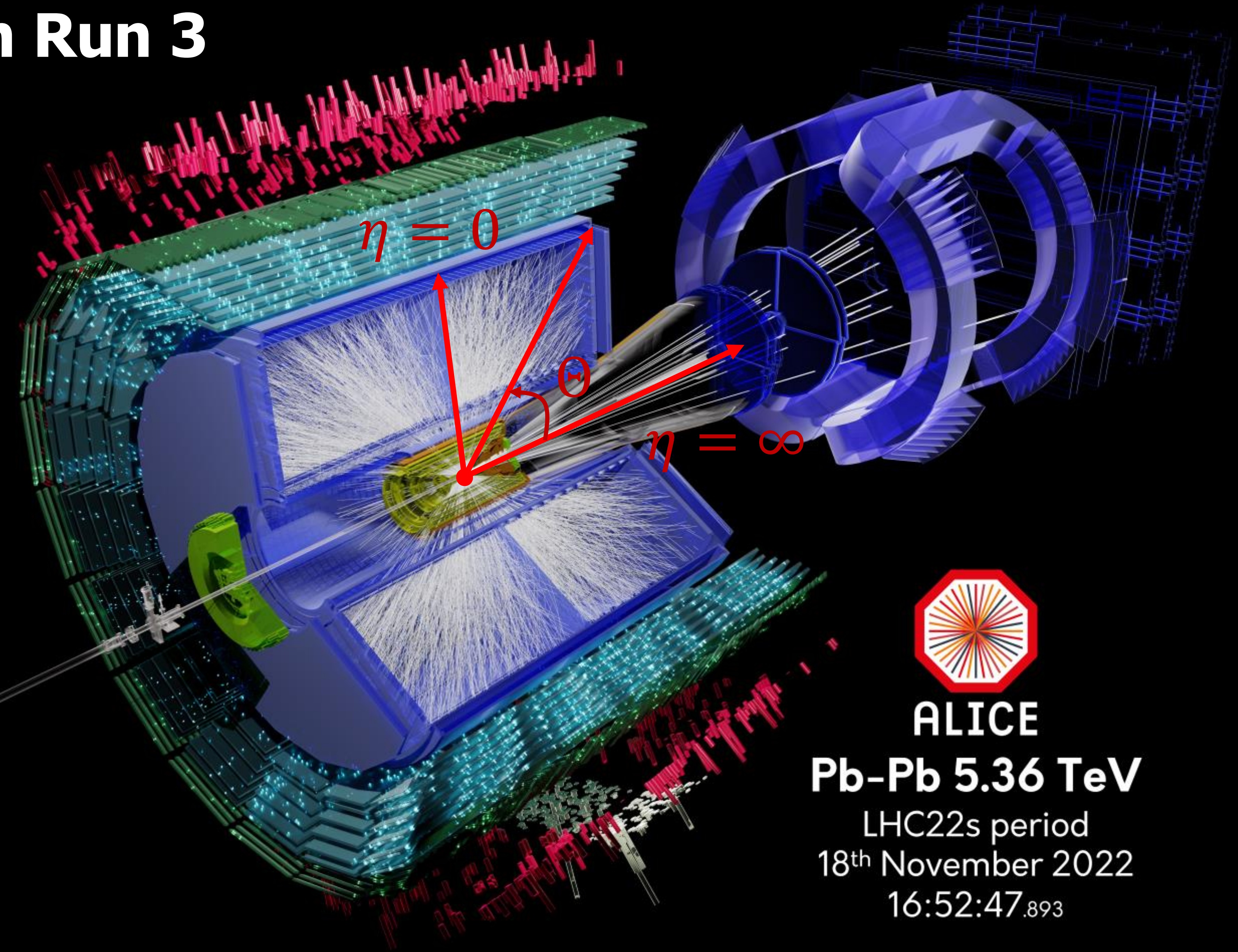

Strangeness enhancement phenomenon

Strangeness originally proposed as a signature of QGP

QGP

Strangeness enhancement phenomenon

Strangeness originally proposed as a signature of QGP

QGP → deconfinement

Strangeness enhancement phenomenon

Strangeness originally proposed as a signature of QGP

QGP → deconfinement → lower effective s quark mass

Strangeness enhancement phenomenon

Strangeness originally proposed as a signature of QGP

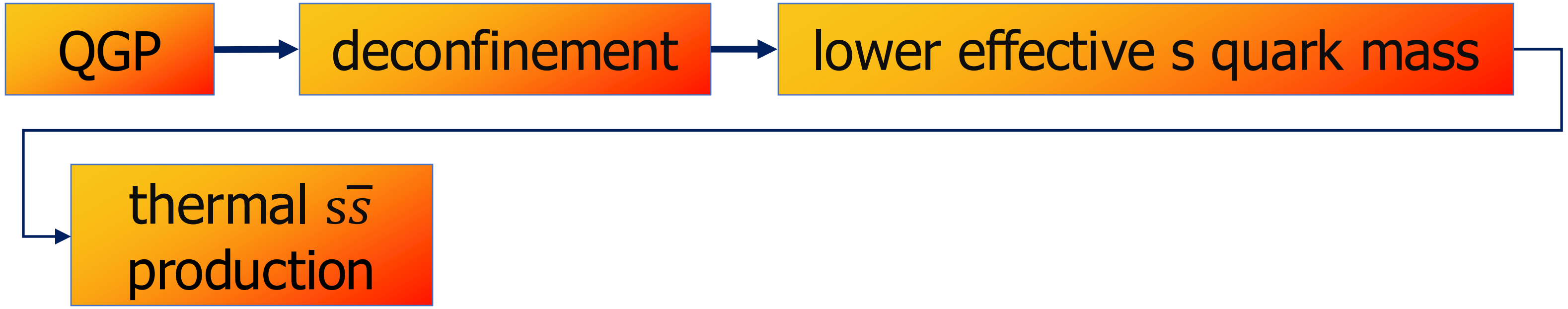

Strangeness enhancement phenomenon

Strangeness originally proposed as a signature of QGP

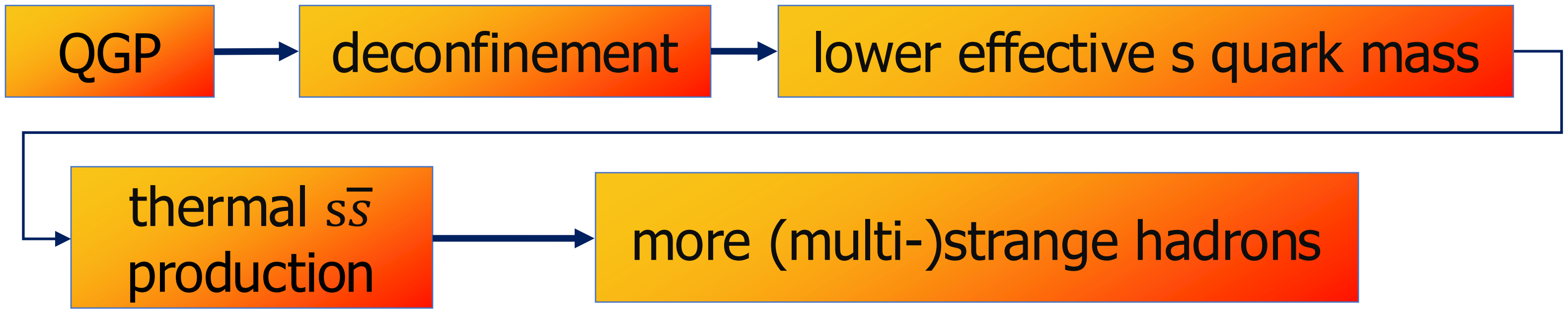

Strangeness enhancement phenomenon

Strangeness originally proposed as a signature of QGP

QGP → deconfinement → lower effective s quark mass → thermal $s\bar{s}$ production → more (multi-)strange hadrons

Strangeness enhancement phenomenon

Strangeness originally proposed as a signature of QGP

QGP → deconfinement → lower effective s quark mass → thermal $s\bar{s}$ production → more (multi-)strange hadrons

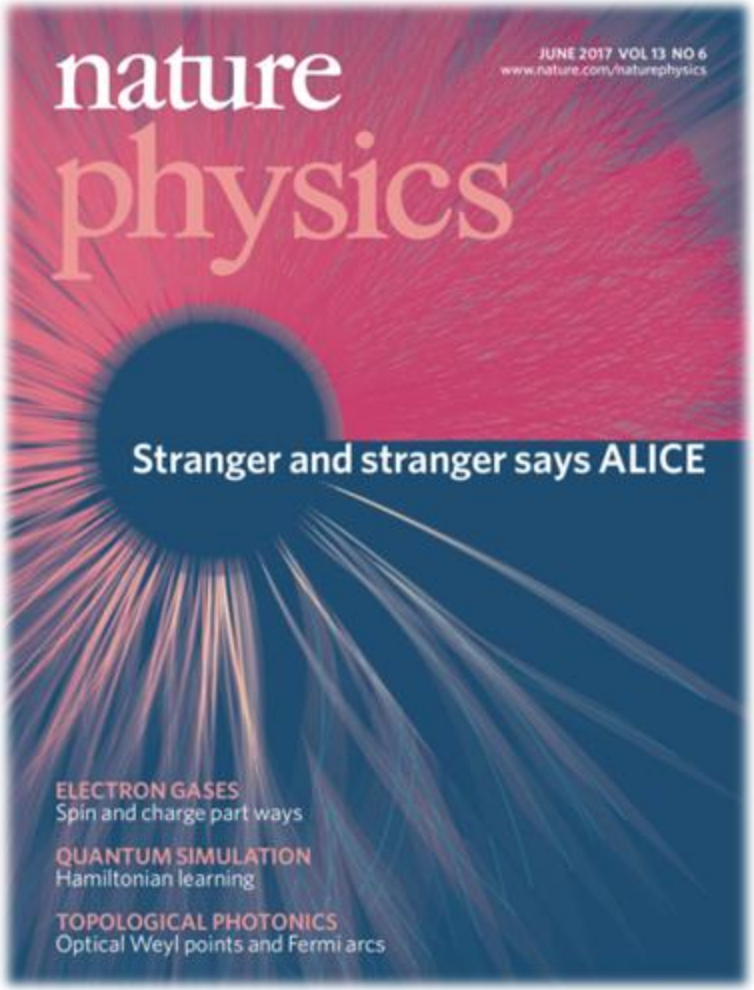

Nature Physics 13, 535 (2017)

Strangeness enhancement phenomenon

Strangeness originally proposed as a signature of QGP

QGP → deconfinement → lower effective s quark mass → thermal $s\bar{s}$ production → more (multi-)strange hadrons

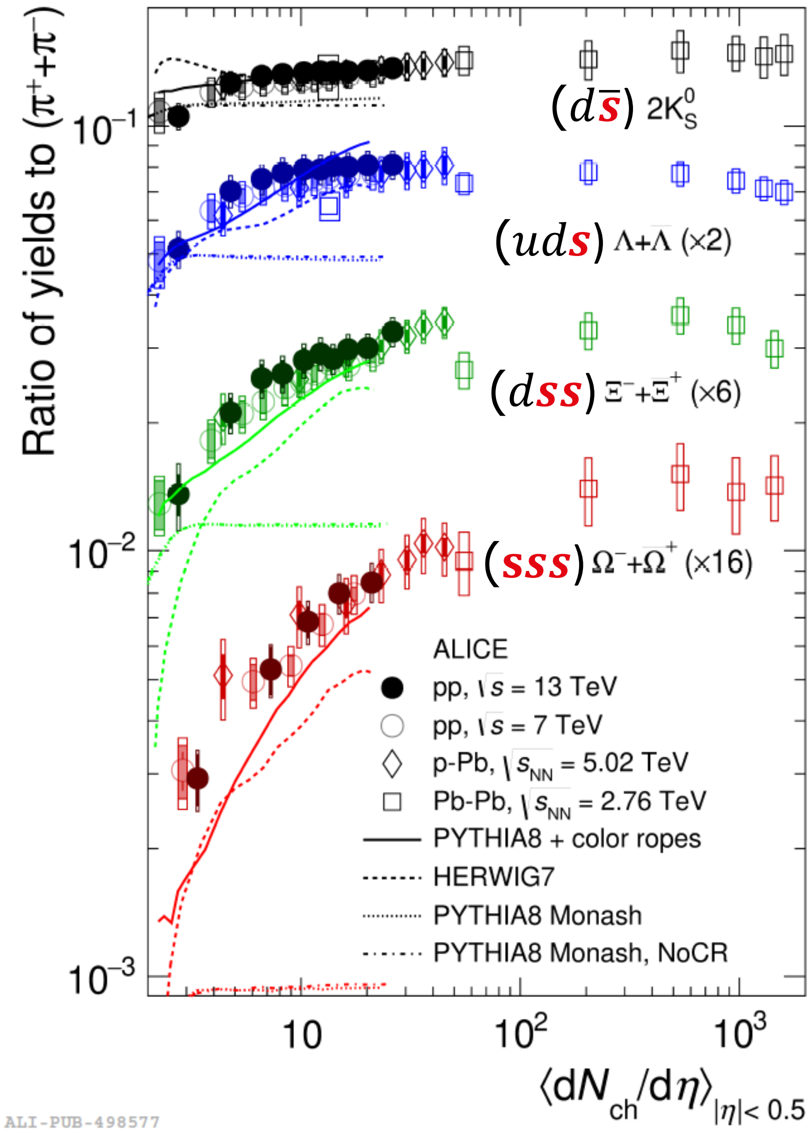

Eur. Phys. J. C 80, 693 (2020)

Strangeness reconstruction with ALICE

Art by H. Herde

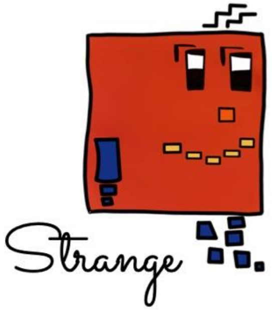

The identification of (multi-)strange hadrons is based on two topologies:

V^0: neutral particle decaying weakly into a pair of charged particles (V-shaped decay)

$$(d\bar{s}) \quad K^0_S \rightarrow \pi^+ + \pi^-$$

$$(uds) \quad \Lambda\,(\bar{\Lambda}) \rightarrow p\,(\bar{p}) + \pi^-\,(\pi^+)$$

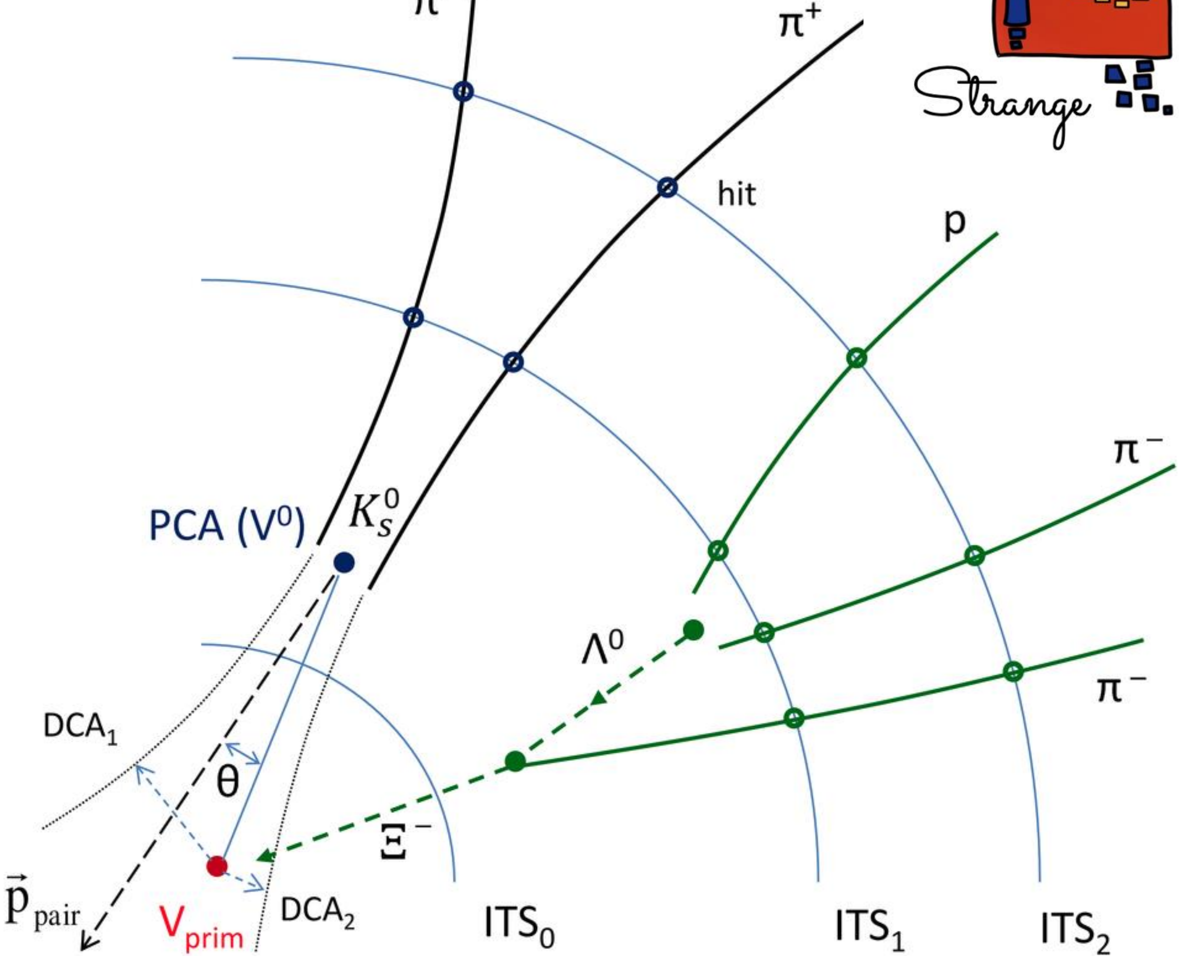

Strangeness reconstruction with ALICE

Art by H. Herde

The identification of (multi-)strange hadrons is based on two topologies:

V^0: neutral particle decaying weakly into a pair of charged particles (V-shaped decay)

$$(d\bar{s}) \quad K^0_S \rightarrow \pi^+ + \pi^-$$

$$(uds) \quad \Lambda\,(\bar{\Lambda}) \rightarrow p\,(\bar{p}) + \pi^-\,(\pi^+)$$

Cascade: charged particle decaying weakly into a V^0 + charged particle

$$(dss) \quad \Xi^-\,(\bar{\Xi}^+) \rightarrow \Lambda\,(\bar{\Lambda}) + \pi^-\,(\pi^+)$$

$$(sss) \quad \Omega^-\,(\bar{\Omega}^+) \rightarrow \Lambda\,(\bar{\Lambda}) + K^-\,(K^+)$$

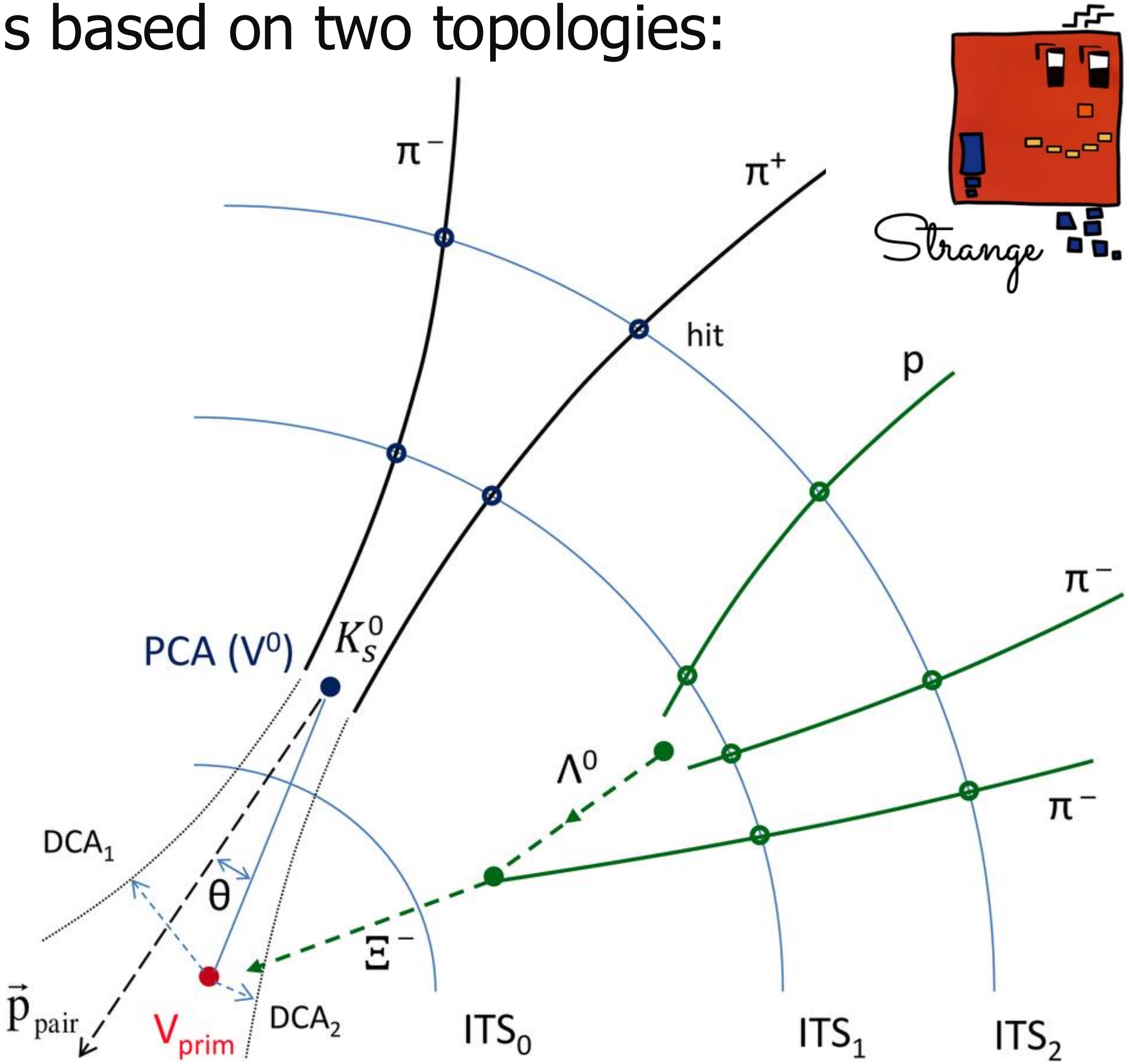

Multiplicity dependent $< p_T >$ of charged particles

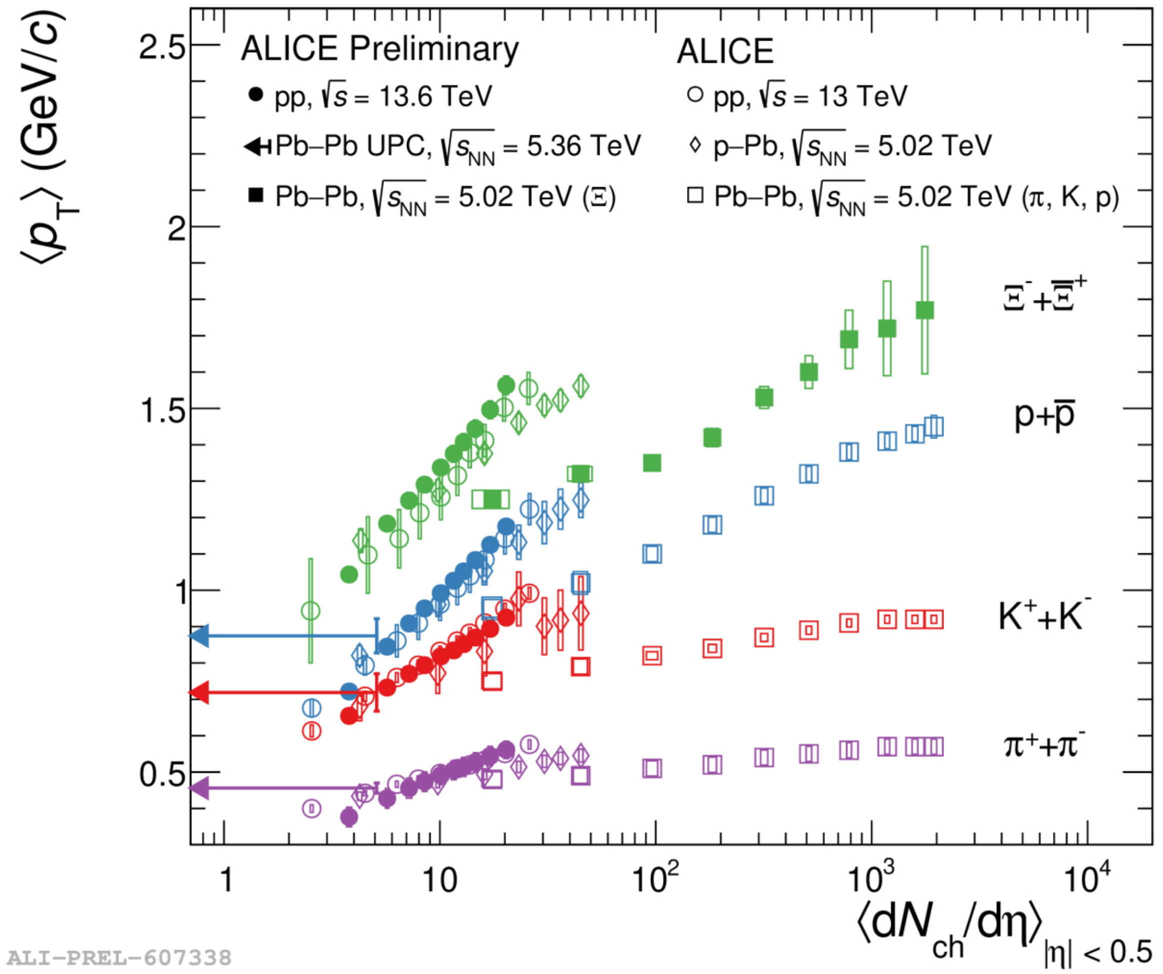

- $< p_T >$ **doesn't connect** between different collision systems

Multiplicity dependent $< p_T >$ of charged particles

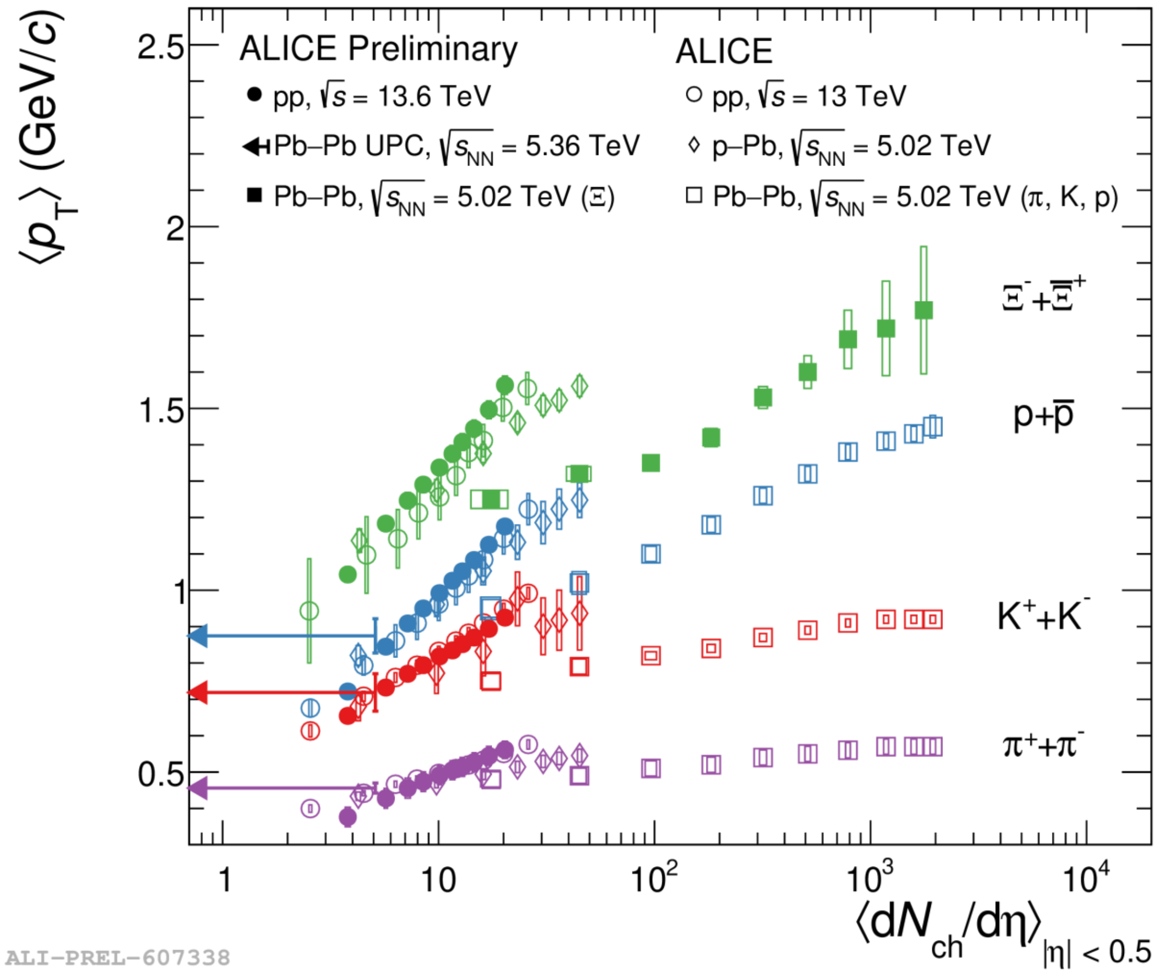

- $< p_T >$ **doesn't connect** between different collision systems

Multiplicity dependent $< p_T >$ of charged particles

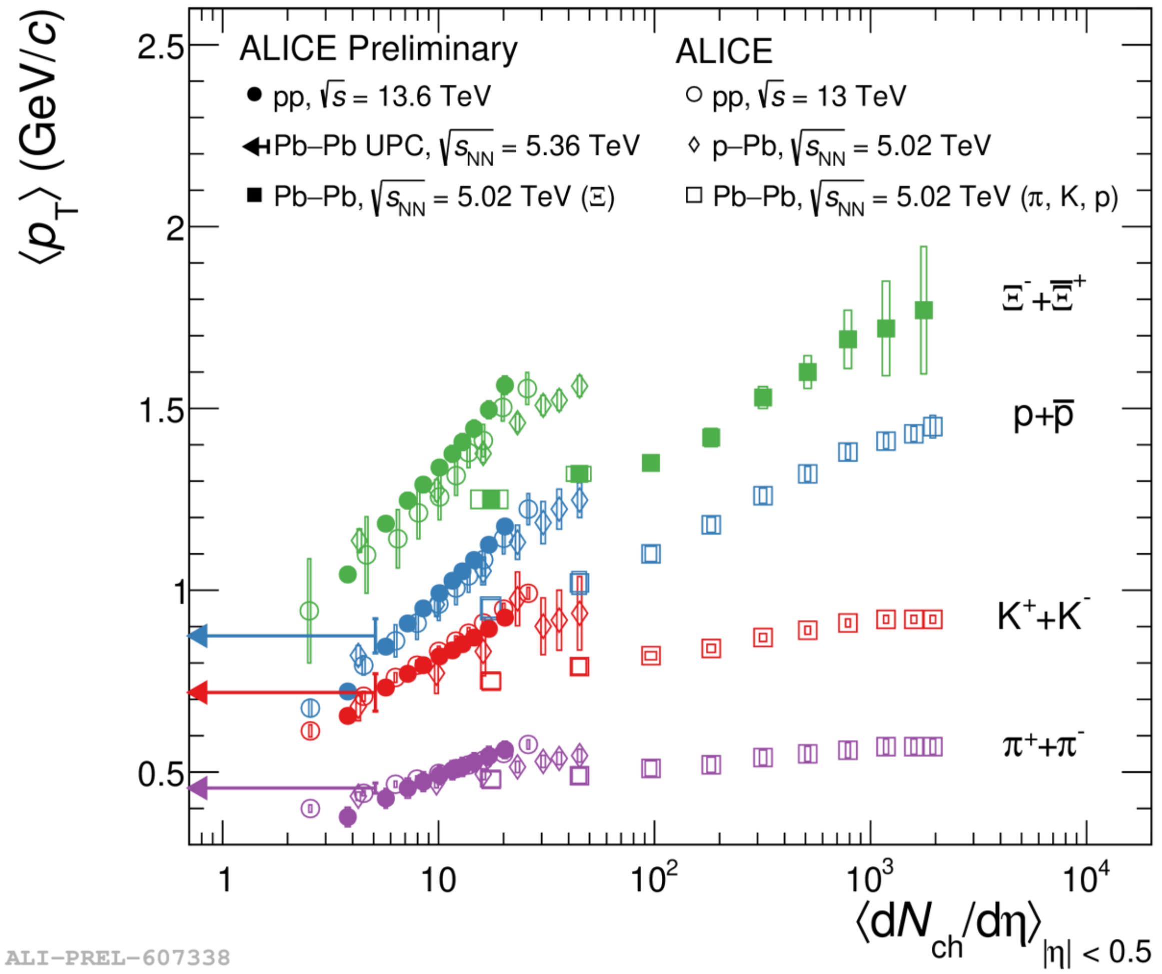

- $< p_T >$ **doesn't connect** between different collision systems

- **Same mid-rapidity activity** in pp and Pb–Pb corresponds to harder spectra in pp
- Influence of **jets** on $< p_T >$ in high-multiplicity pp events

Charged particle production across different systems

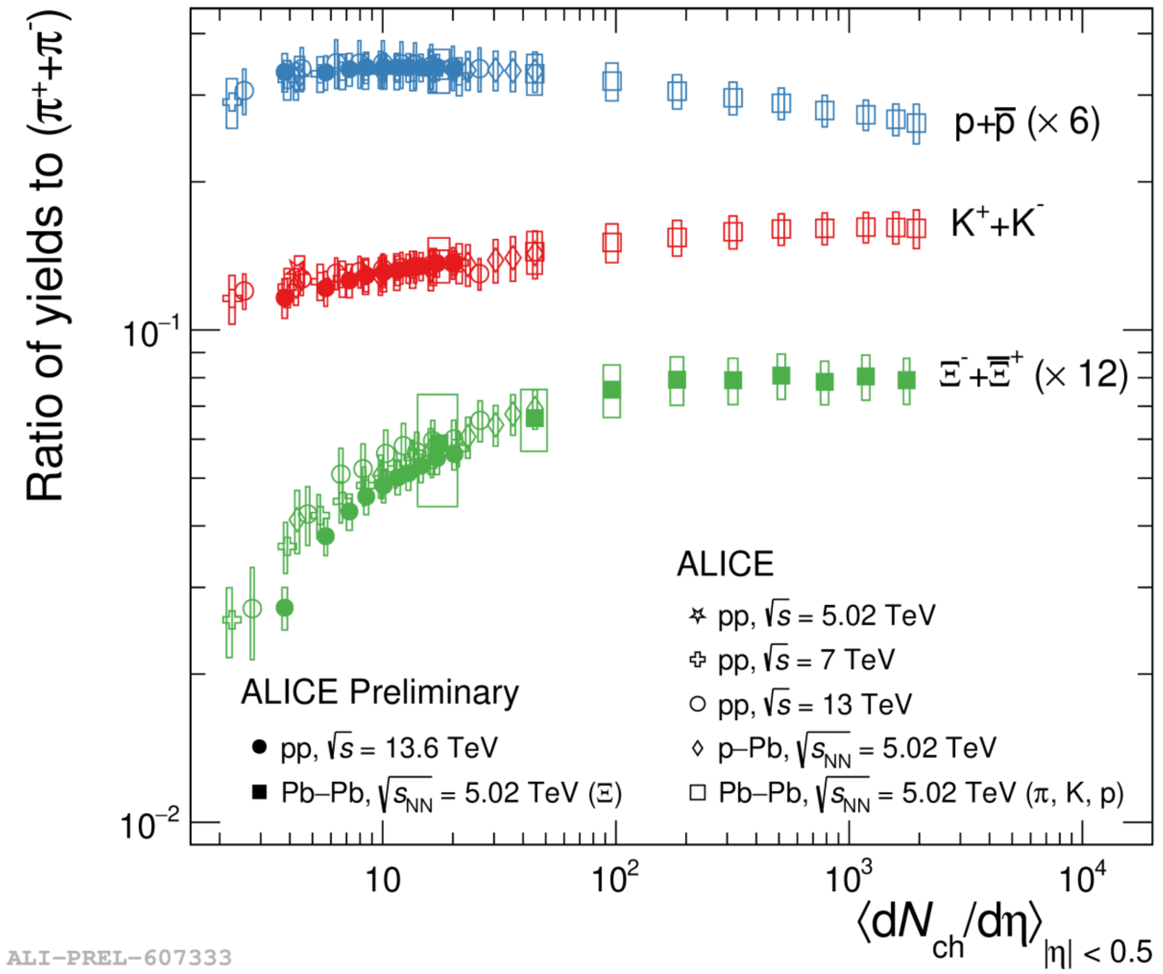

- $< p_{\mathrm{T}} >$ **doesn't connect** between different collision systems

- **Same mid-rapidity activity** in pp and Pb–Pb corresponds to harder spectra in pp

- Influence of **jets** on $< p_{\mathrm{T}} >$ in high-multiplicity pp events

- ALICE preliminary results on **ratio of hadron yields to** $(\pi^{-}+\pi^{+})$ confirm **continuous trend** observed before **starting from low-multiplicity pp** at $\sqrt{s} = 7$ and 13 TeV **up to central Pb–Pb collisions** at $\sqrt{s_{\mathrm{NN}}} = 5.02$ TeV

➡ Hadron yields depend only on the **multiplicity**, while the p_{T} distribution of the formed hadrons is affected by the **hadronizing environment**

Strange hadron dynamics

JHEP09, 006 (2018)

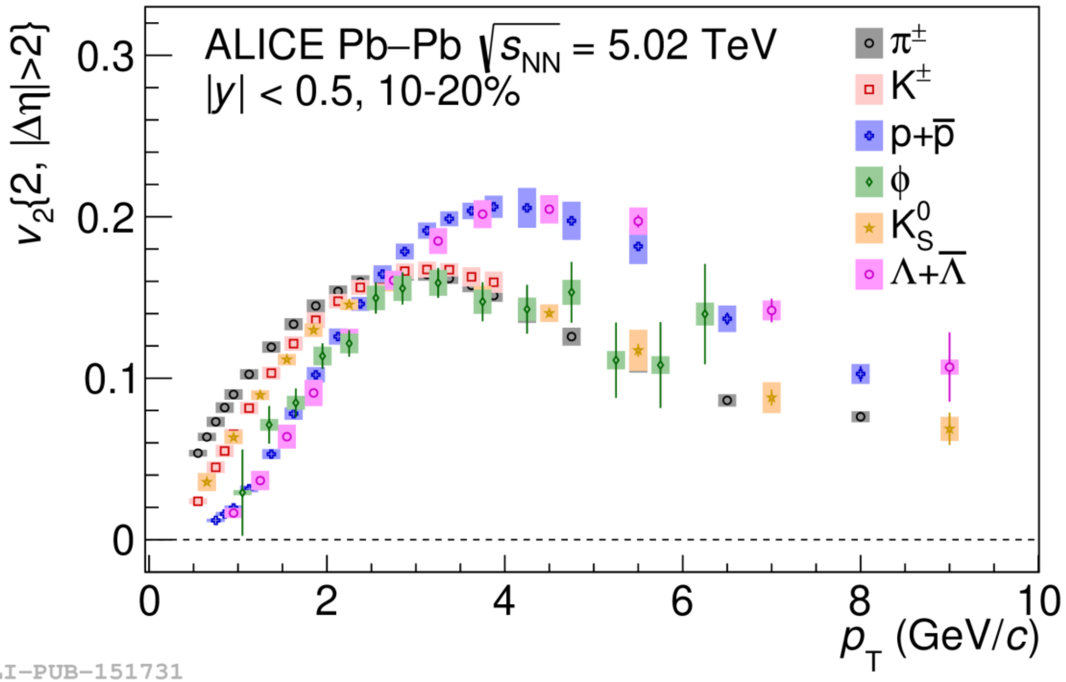

ALI-PUB-151731

Phys. Rev. Lett. 111, 222301 (2013)

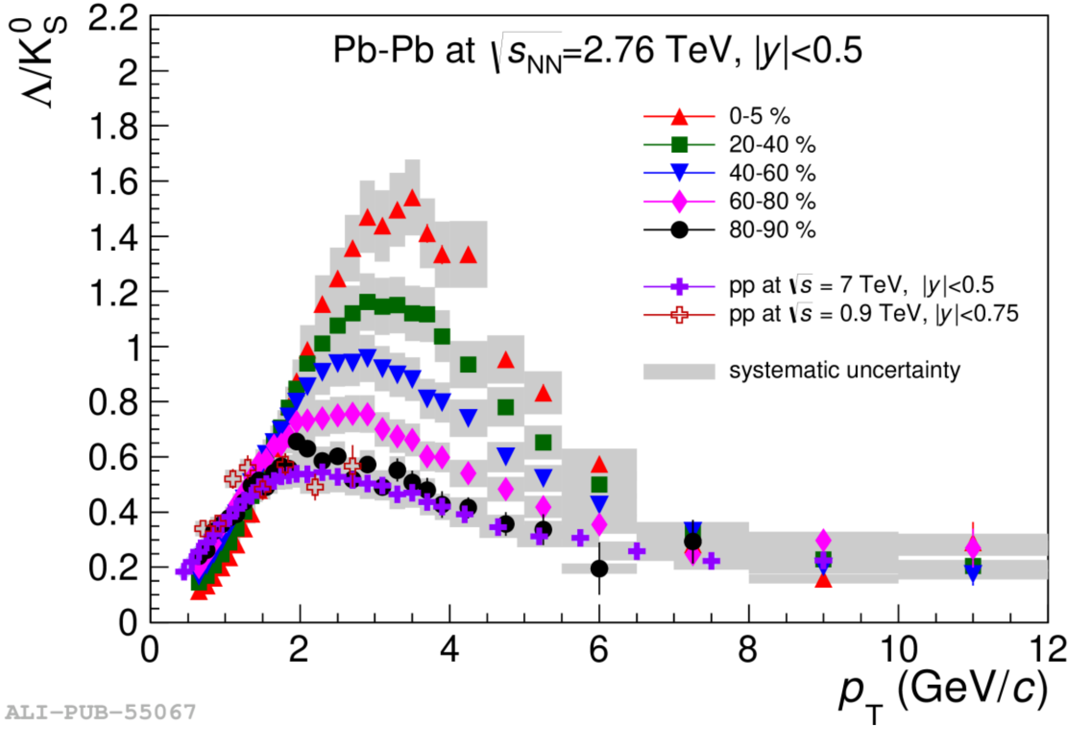

ALI-PUB-55067

Anisotropic flow patterns are characterized using a **Fourier expansion** of the invariant triple differential distribution:

$$E\frac{d^3N}{d^3\boldsymbol{p}} = \frac{1}{2\pi}\frac{d^2N}{p_T dp_T dy}\left(1 + 2\sum_{n=1}^{\infty} v_n cos[n(\varphi - \psi_{RP})]\right)$$

$v_n = \langle cos[n(\varphi - \psi_{RP})]\rangle$

v_1 – directed flow

v_2 – elliptic flow

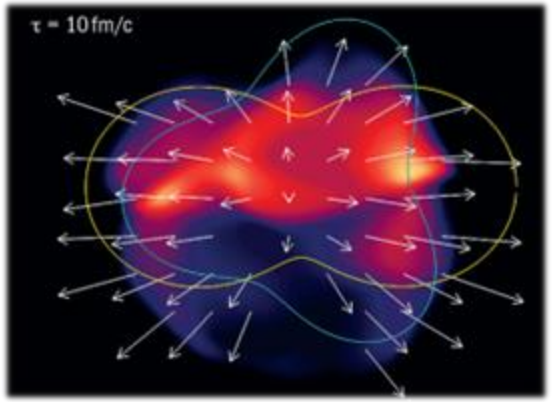

IMAGE: MUSIC

Strange hadron dynamics

[JHEP09, 006 (2018)](#)

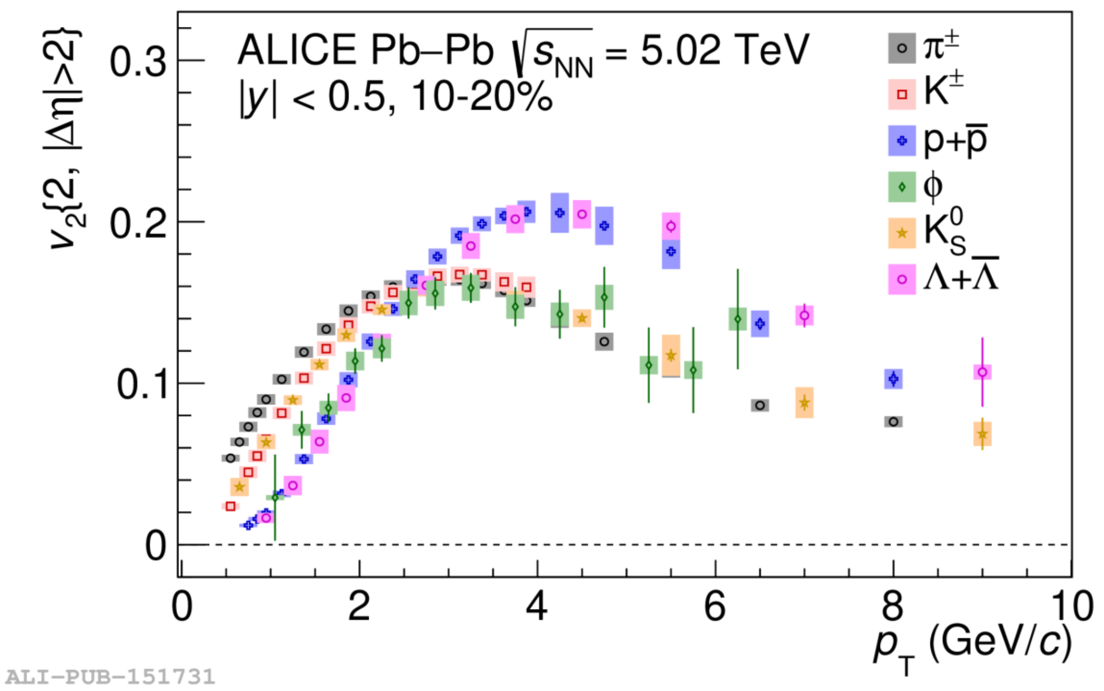

[Phys. Rev. Lett. 111, 222301 (2013)](#)

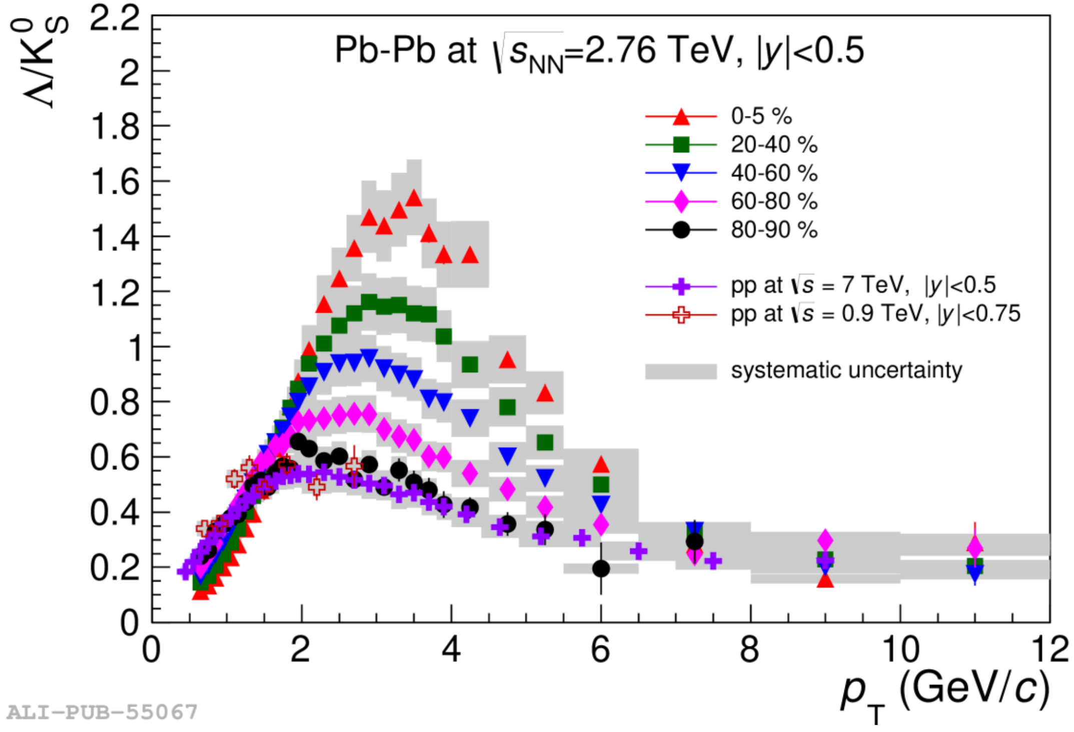

Elliptic flow of strange particles follows **mass ordering** at low p_T and **meson-baryon splitting** at intermediate p_T

➡ Centrality-dependent p_T-spectra **hardening** & baryon/meson ratio **enhancement** at intermediate p_T can be explained by radial flow and/or color reconnection

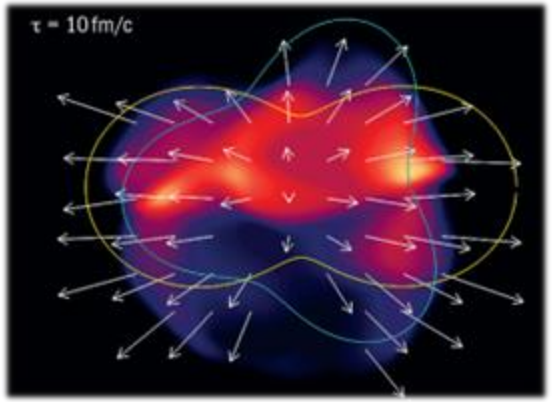

IMAGE: MUSIC

QGP in small systems?

- **ALICE** studies suggest that small systems, such as proton-nucleus and even proton-proton collisions, may also exhibit QGP-like behavior [1, 2]
- Study of strangeness production in small systems, where no QGP is expected, can help to **disentangle initial-state** effects from **QGP-driven** phenomena
- Recent **ATLAS** studies reveal signatures of collectivity in **photo-nuclear UPC Pb–Pb collisions!**

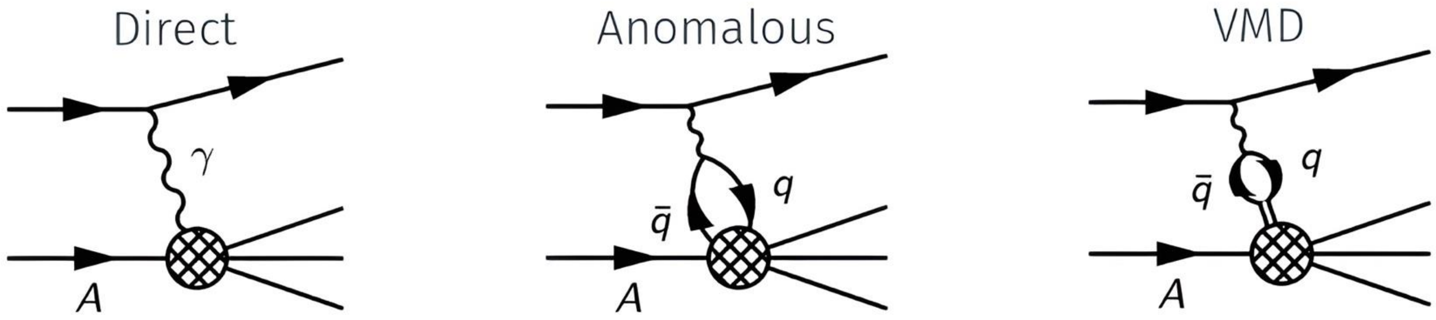

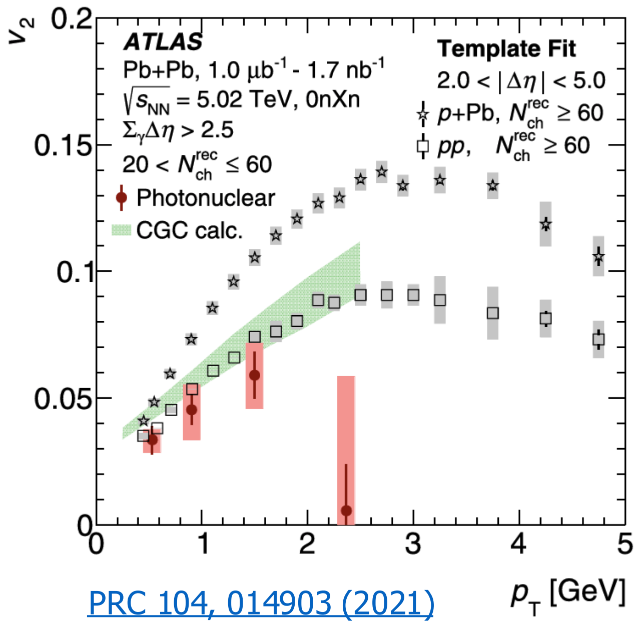

PRC 104, 014903 (2021)

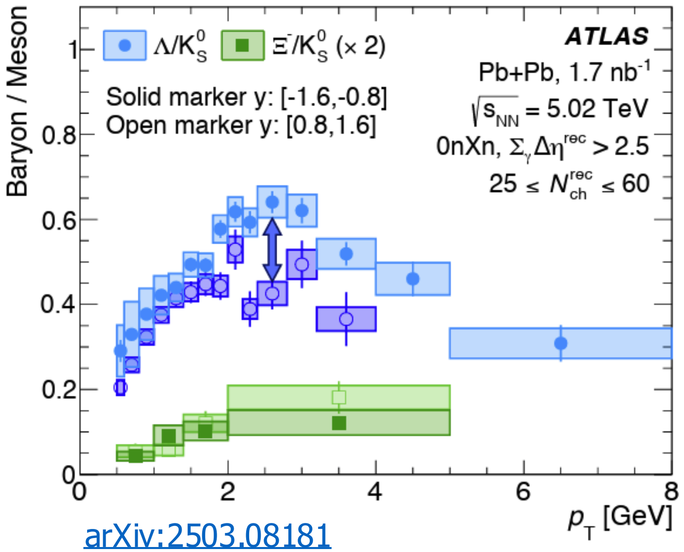

arXiv:2503.08181

[1] PLB 728, 24 (2014)
[2] Nature Physics 13.6, 535 (2017)

Ultra-peripheral collisions

[1] E. Fermi, Nuovo Cimento 2, 143-155 (1925)
[2] C.F. von Weizsacker, Z. Phys. 88, 612 (1934)

- **Ultra-peripheral collisions** (UPCs) occur at large impact parameters ($b > b_{\min} = 2R$)
- The large Lorentz contraction of ultra-relativistic ions creates extremely concentrated electromagnetic fields ($\vec{E}$ and $\vec{H}$)
- The quanta of these fields, photons, travel in the $\vec{E} \times \vec{H}$ direction and are parallel to the ion velocity [1, 2]
- Photon flux in $v \to c$ limit can be written as

$$\frac{dN_\gamma}{dE_\gamma} = \alpha_{\mathrm{EM}} \frac{Z^2}{E_\gamma}\left(xK_0(x)K_1(x) - \frac{1}{2}x^2\left(K_1^2(x) - K_0^2(x)\right)\right)$$

where $x = \frac{E_\gamma b_{\min}}{\gamma}$ and α_{EM} is a structure constant

$K_n(x)$ are the n[th] Bessel's functions of the 2[nd] kind

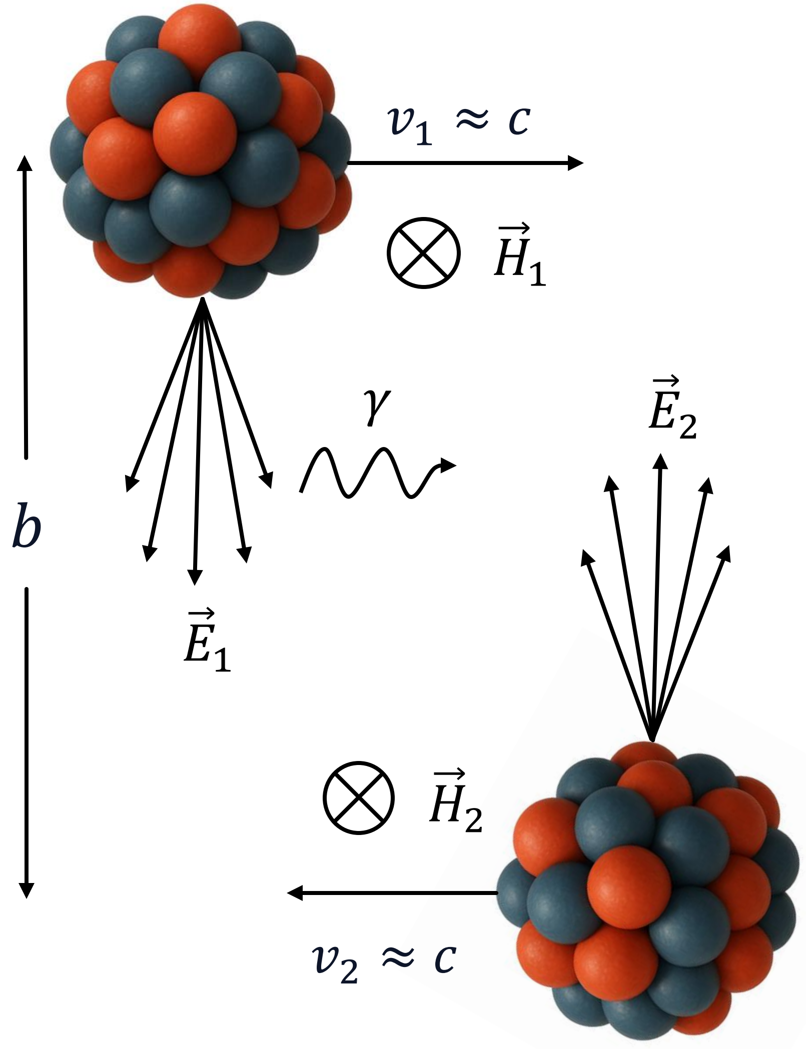

Baryon-to-meson ratio in UPCs

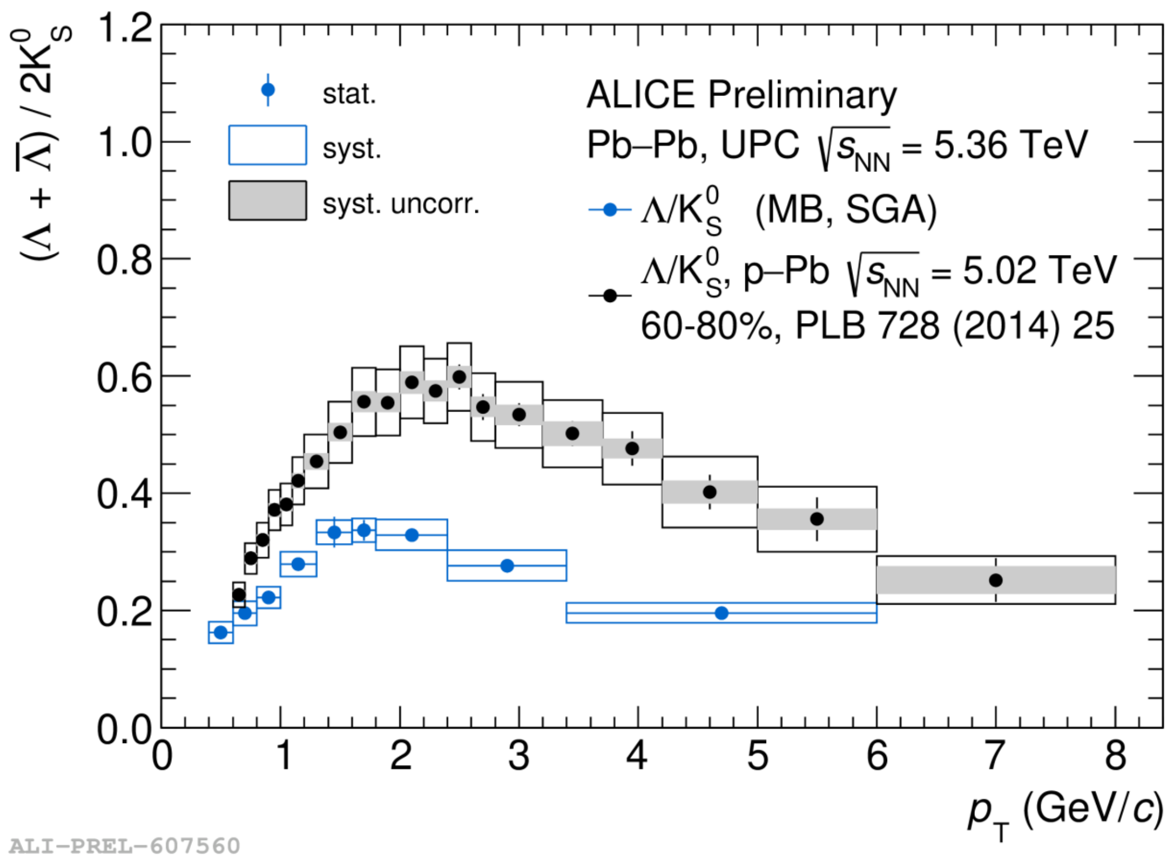

- The enhancement of Λ/K^0_S observed in SG photo-nuclear collisions at p_T ~ 2 GeV/c is qualitatively reminiscent of that measured in low-multiplicity p–Pb ($\langle {}^{dN_{ch.}}/_{d\eta} \rangle_{|\eta_{lab}|<0.5} = 9.8 \pm 0.2$)

Baryon-to-meson ratio in UPCs

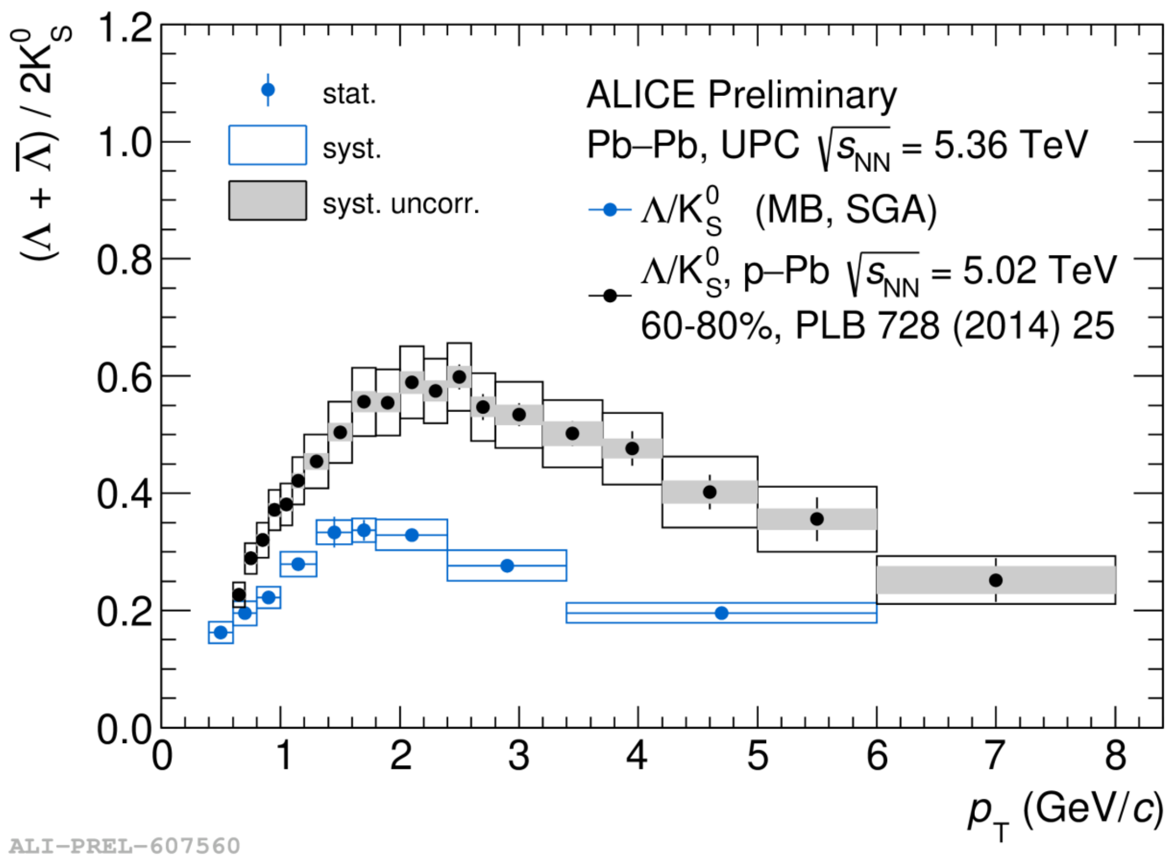

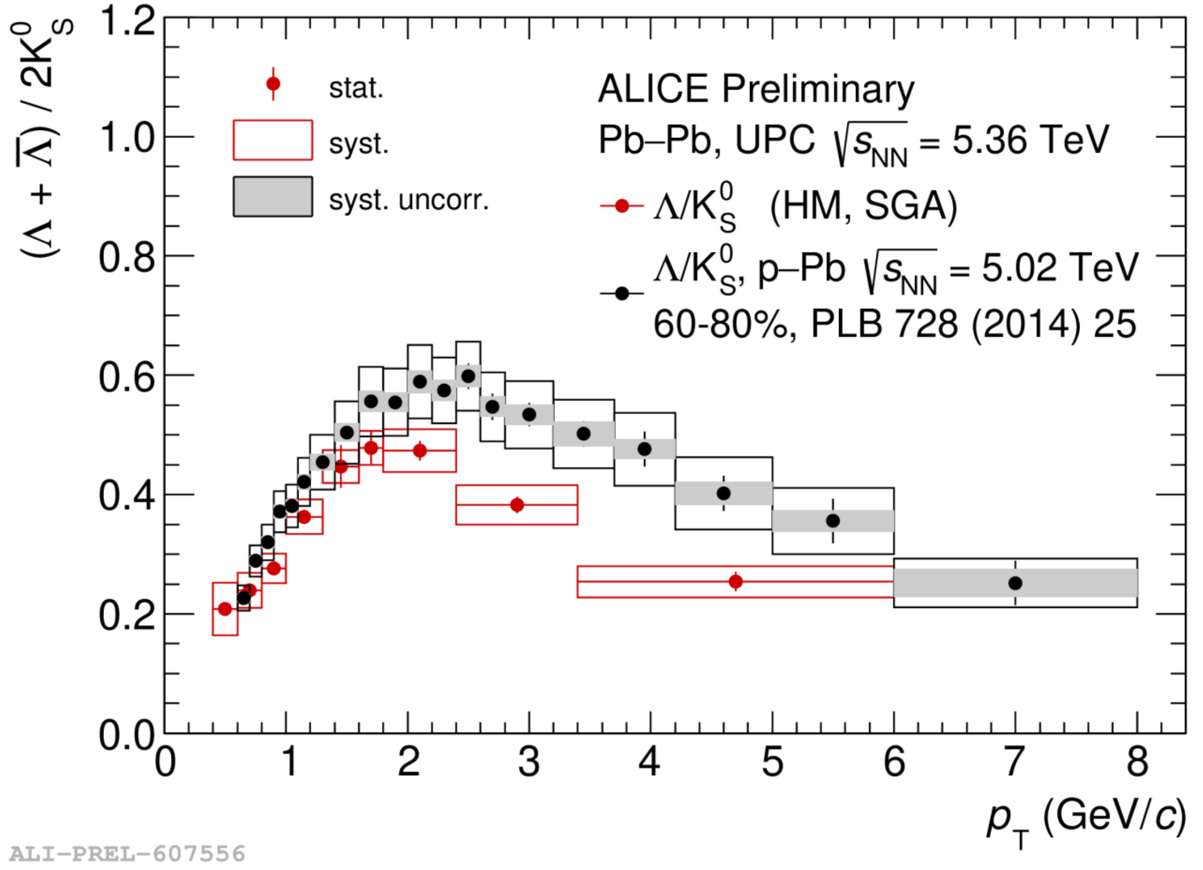

- The enhancement of Λ/K^0_S observed in SG photo-nuclear collisions at $p_T \sim$ 2 GeV/c is qualitatively reminiscent of that measured in low-multiplicity p–Pb ($\langle {}^{dN_{ch.}}/_{d\eta} \rangle_{|\eta_{lab}|<0.5} = 9.8 \pm 0.2$)
- The ratio increases and approaches values measured in low-multiplicity p–Pb as one moves to higher multiplicity event class ($\mathrm{MB} \rightarrow \mathrm{HM}$)

Baryon-to-meson ratio

ATLAS results (high multiplicity)

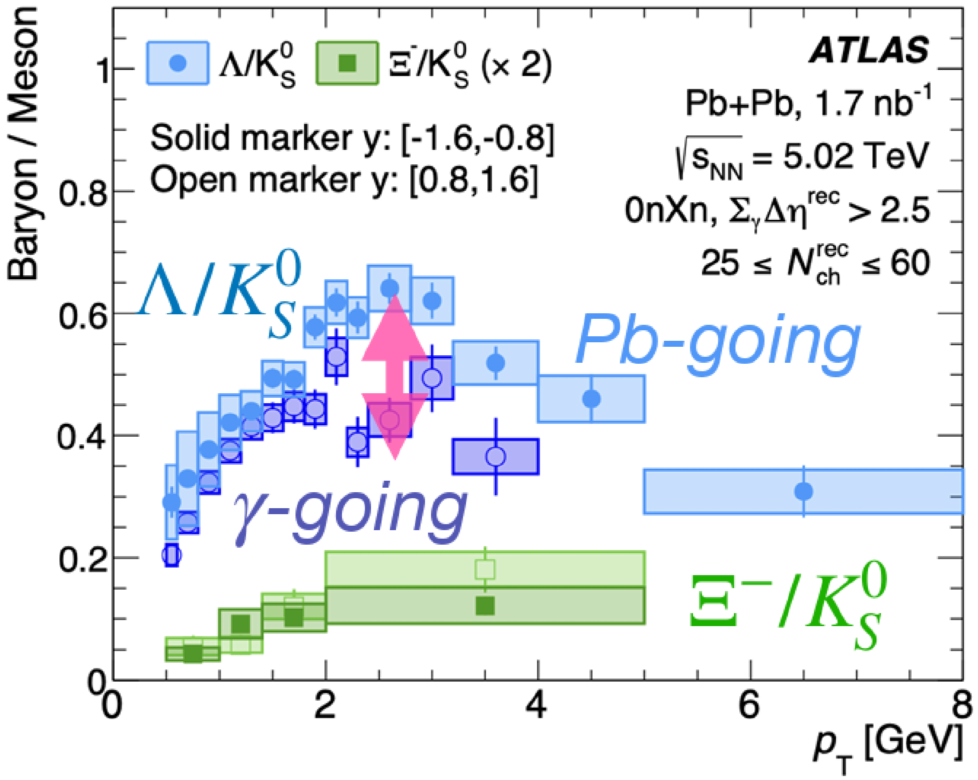

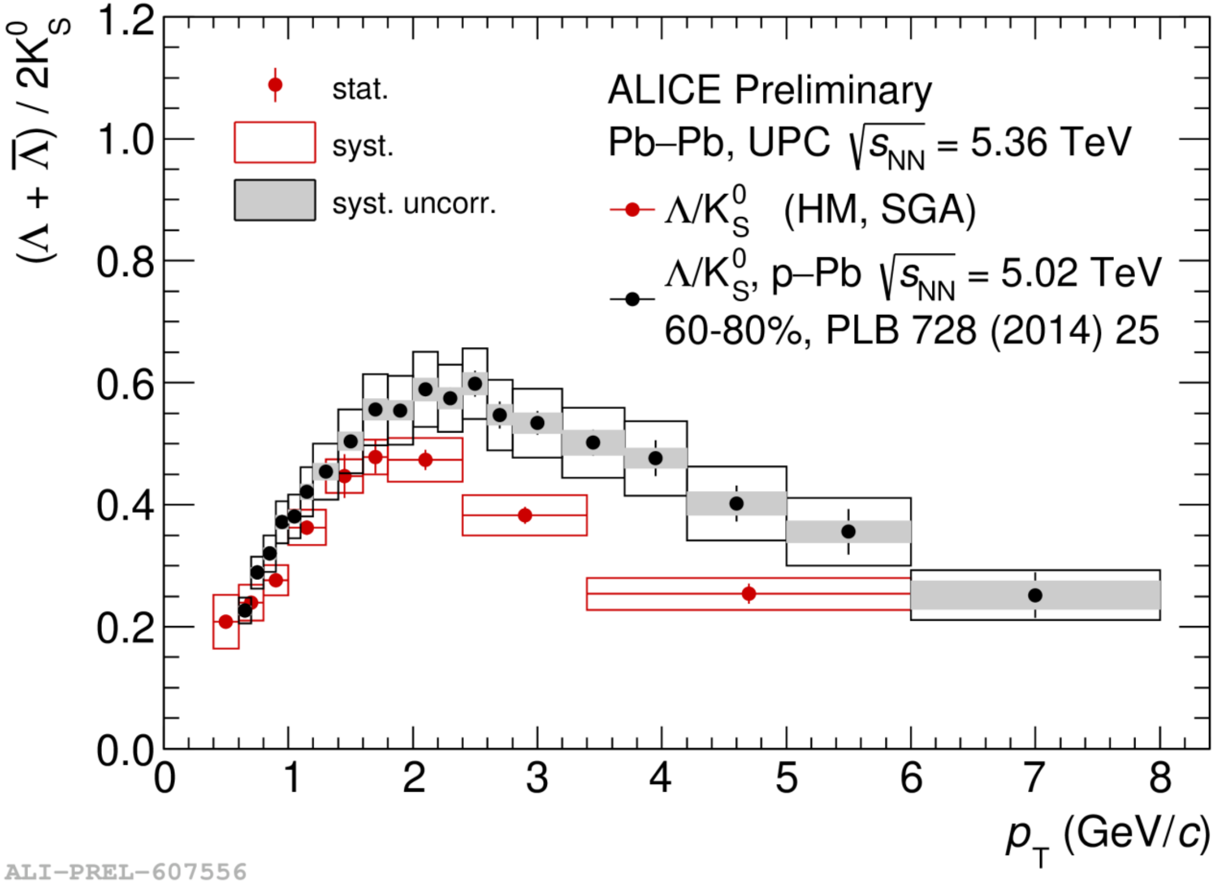

- Similar magnitude of QGP-like signals as in ATLAS results
- γ–Pb collisions are dominated by vector meson dominance, making them effectively equivalent to hadronic vector meson + Pb collisions
- Results pose a clear challenge to existing theoretical models

ALICE ITS3 upgrade

ITS2 – largest pixel detector built:
- 24k chips, 12.5 GPixel
- 10 m^2, 0.364% X_0 per layer

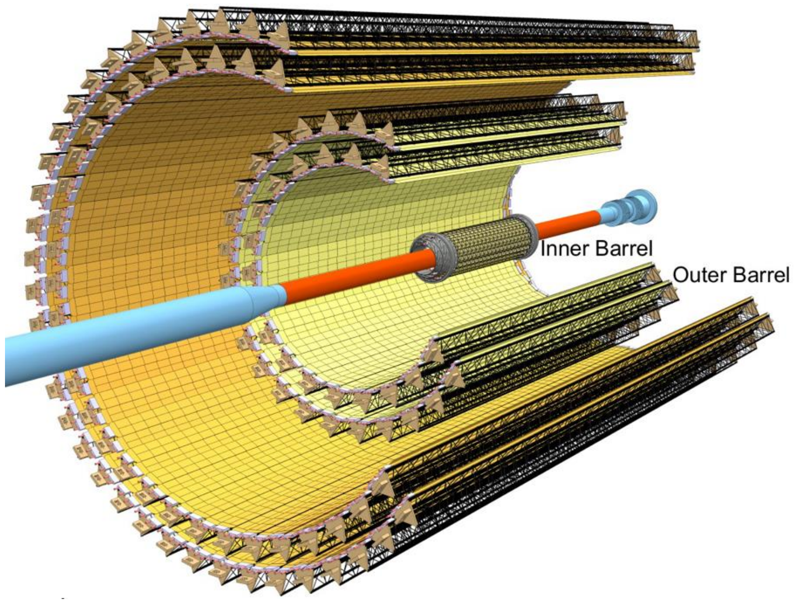

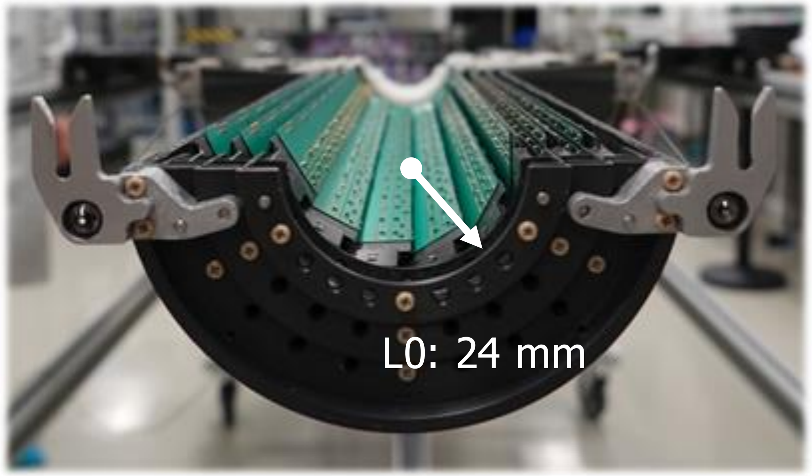

ITS2 Inner Barrel

ALICE ITS3 upgrade

ITS2 – largest pixel detector built:
- 24k chips, 12.5 Gpixel
- 10 m^2, 0.364% X_0 per layer

ITS2 to ITS3 upgrade:
- Replacement of the 3 innermost layers for ALICE Run4
- Beam pipe radius:
  18 mm → 16.5 mm
- Innermost layer radius:
  24 mm → 19 mm

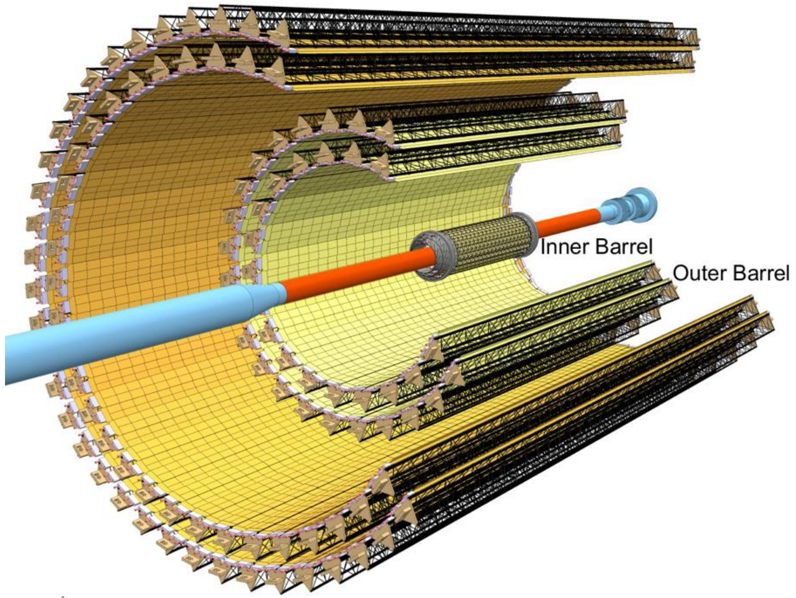

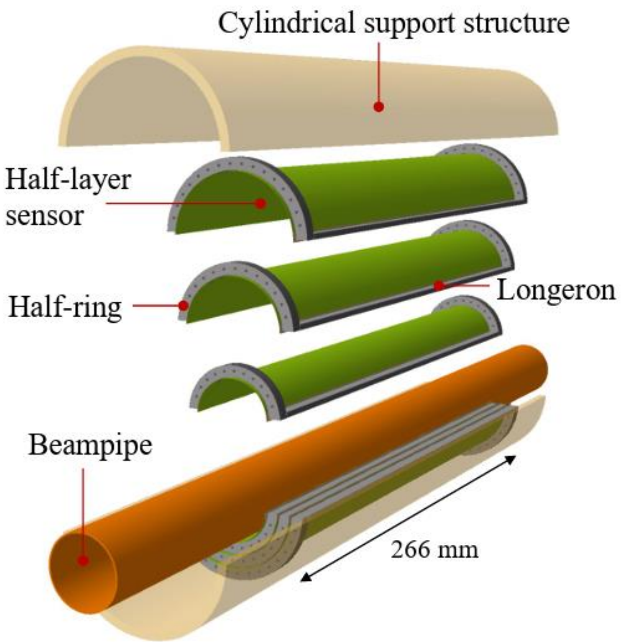

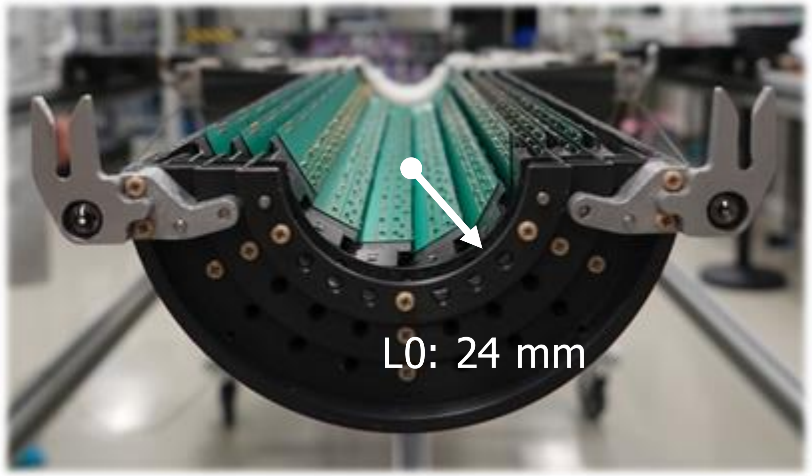

ITS2 Inner Barrel

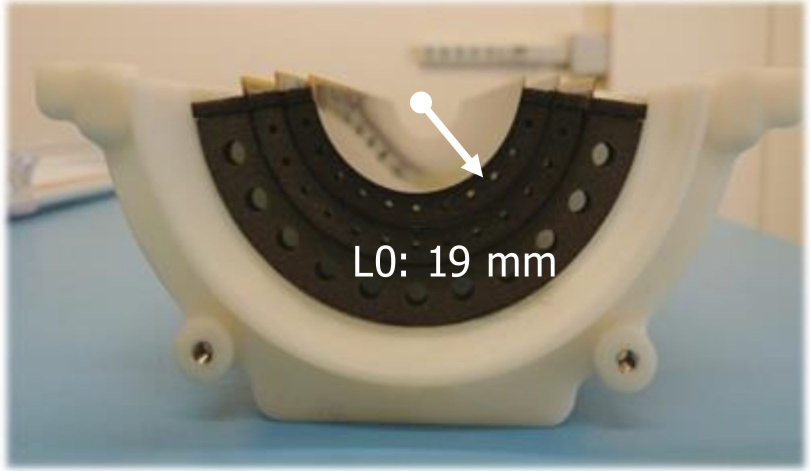

ITS3 Engineering Model

ITS3 TDR - CERN-LHCC-2024-003

ALICE ITS3 upgrade

ITS2 – largest pixel detector built:
- 24k chips, 12.5 Gpixel
- 10 m^2, 0.364% X_0 per layer

ITS2 to ITS3 upgrade:
- Replacement of the 3 innermost layers for ALICE Run 4
- Beam pipe radius:
  18 mm → 16.5 mm
- Innermost layer radius:
  24 mm → 19 mm

ITS3 – 6 wafer-scale MAPs → half layers!
- Cylindrical layers by bending 50 µm silicon sensors
- Up to 98 × 266 mm^2 (stitching technology)
- Reduced average material budget of 0.09% X_0 per layer
- Air cooling

ITS3 TDR - CERN-LHCC-2024-003

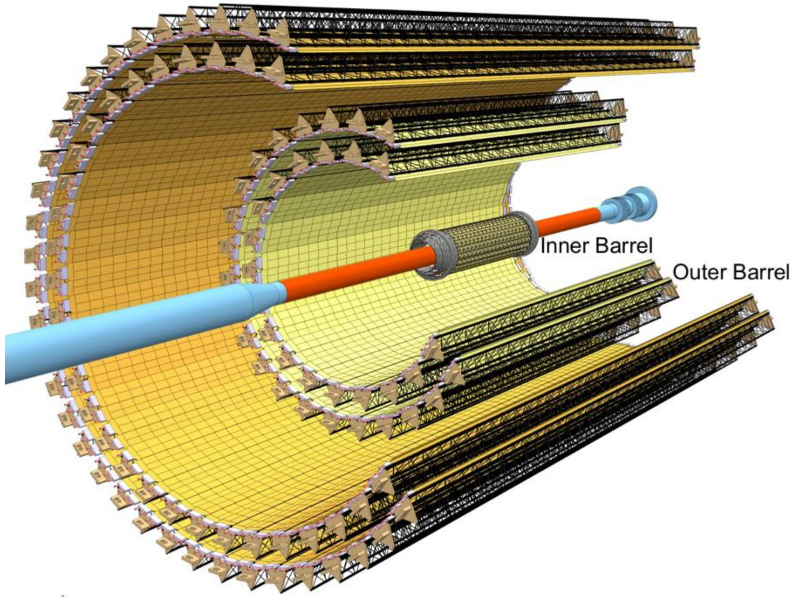

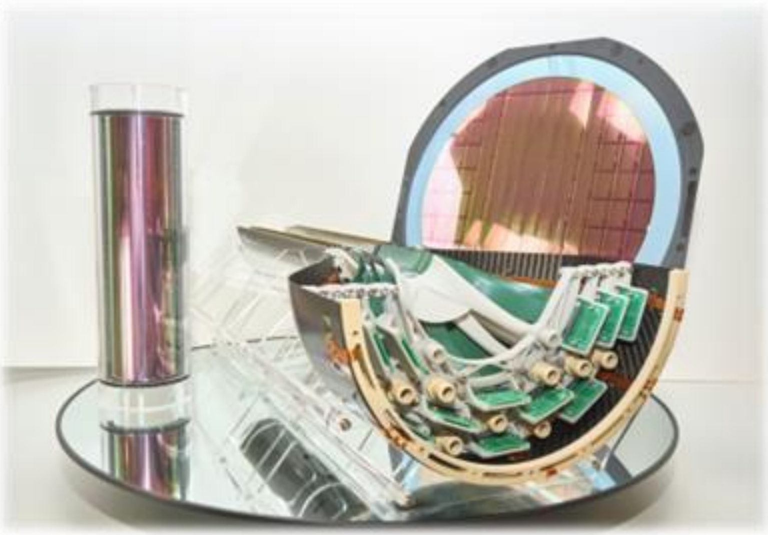

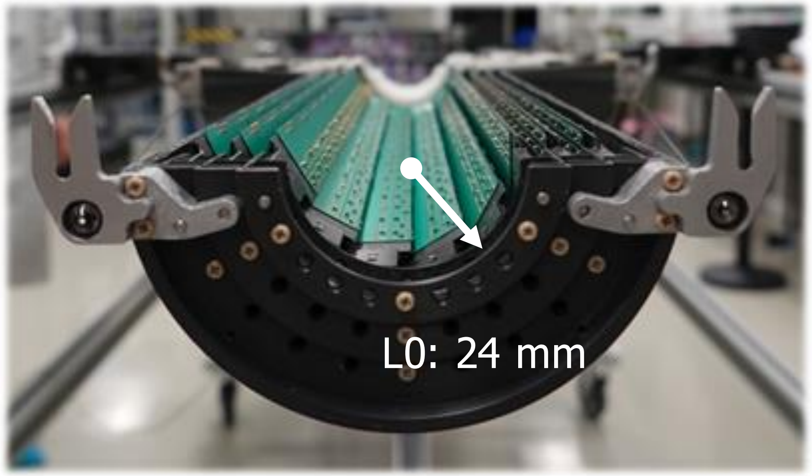

ITS2 Inner Barrel

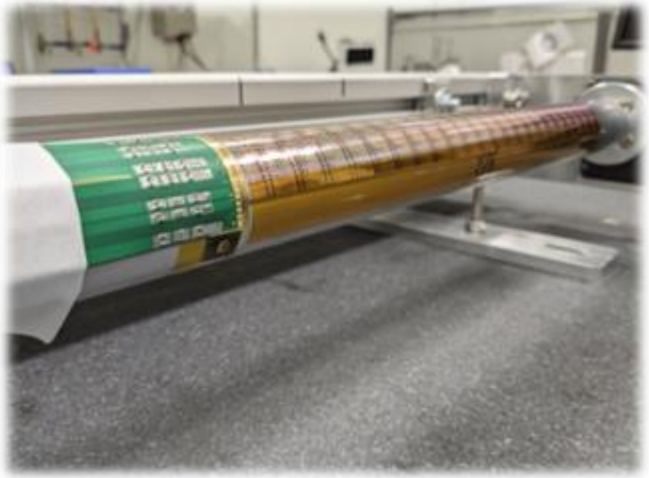
ITS3 Engineering Model

Chip characterization

Latest test beam program
@ Proton Synchrotron (PS)
3-10 September 2025:

- Threshold scans
- Tracking resolution
- Detection efficiency
- In-pixel efficiency
- Parameter scans
- Time-over-threshold measurements (TOT)
- Testing of different detector designs

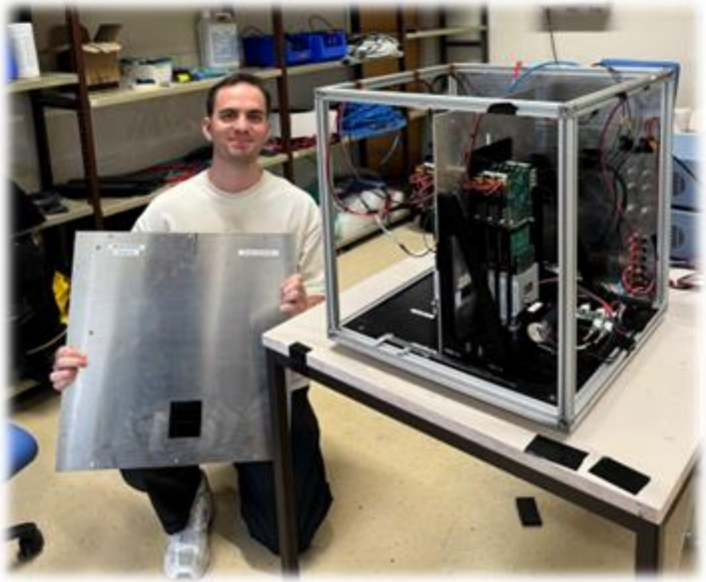

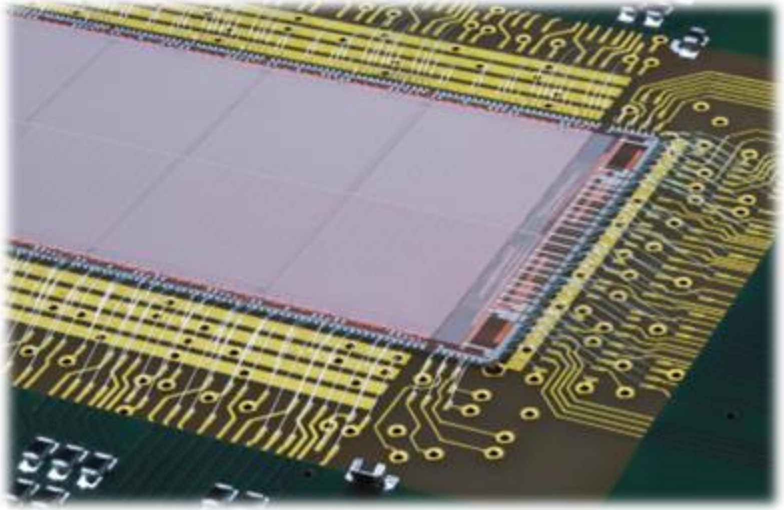

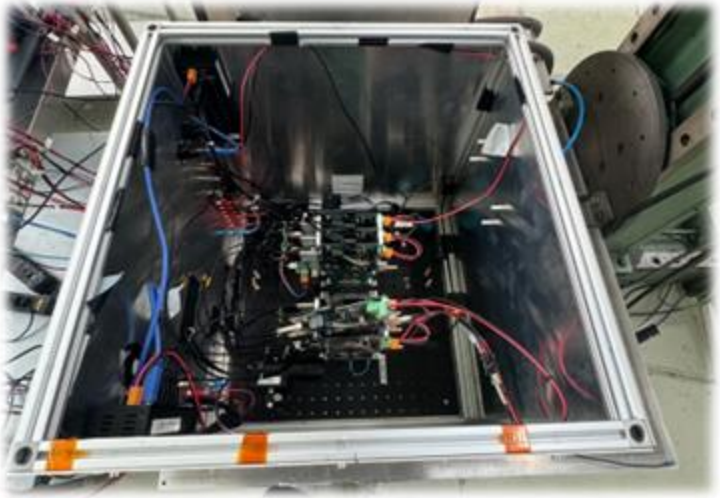

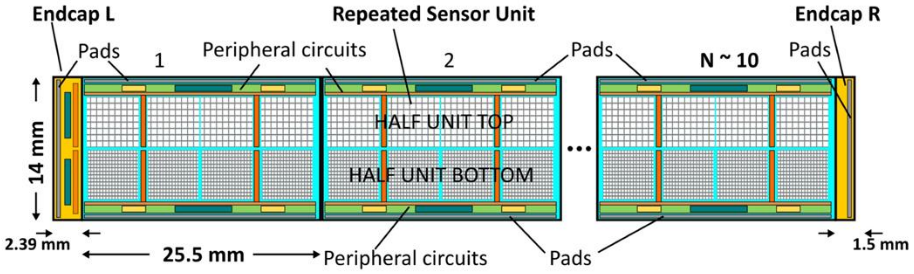

Summary

- Fruitful 3 years of active broad range research within ALICE
- It was shown that strange hadron yields depend only on multiplicity, while the $< p_{\mathrm{T}} >$ distributions of the formed hadrons are influenced by the hadronizing environment
- The study was extended to ultra-peripheral Pb–Pb collisions, the smallest and cleanest system available at the LHC
- Signs of collectivity were observed, consistent with recent ATLAS results
- In parallel, development and testing of ITS3 detector chips as part of future hardware upgrades is being carried out

Thank you for attention!